VIRGINIA POLYTECHNIC INSTITUTE
AND STATE UNIVERSITY

The Charles E. Via, Jr. Department
of Civil and Environmental Engineering
Blacksburg, VA 24061

Structural Engineering and Materials

Rotational and Translational Stiffness Provided by Insulated Metal Panels to Girts and Purlins in Metal Building Wall and Roof Systems

by

Haiteng Wu
Graduate Research Assistant

Cristopher D. Moen, Ph.D., P.E.
Associate Professor

Report No. CE/VPI-ST-15-03

February 2016

Table of Contents

1 Introduction and background

The design of buildings is often compartmentalized due to the disparate nature of the different systems that make up a finished structure. Building mechanical, electrical, plumbing, environmental, and structural systems are often designed by separate design groups with little consideration for the beneficial interaction between components of different systems. Recent strengthening of energy code requirements has resulted in more widespread use of thermal insulation in the form of insulated metal panels (IMPs) in an effort to meet the increasing demand for energy efficiency. These panels are comprised of a solid core of insulating material such as polyurethane or polyisocyanurate surrounded by thin metal panels and molded together as a single unit. As a result of their sandwich-like construction, these panels exhibit greater stiffness than single-skin thin metal panels, and this greater stiffness can be utilized to provide additional lateral-torsional buckling restraint to the secondary members supporting the panel loads.

The goal of this study is to quantify the restraint provided by IMPs to girts and purlins in a metal building wall and roof system such as that shown in Figure 1. These panels are fastened to their support members with screws that are either uniformly spaced across the panel width and penetrate through the entire panel thickness or that fasten through clips concealed within the side joint located at the panel side edges only. Current through-fastened panel design methodology in the American Iron and Steel Institute (AISI) North American Specification for the Design of Cold-Formed Steel Structural Members does not provide guidance for secondary member design when these panels are employed, thus each new IMP product requires costly testing as part of a wall or roof system in a vacuum chamber.

Figure 1. Metal building with insulated metal panels being installed (courtesy: Stellar)

The results of an experimental program are described in the following chapters that provide rotational and translational spring stiffness (Figure 2) for 6 IMP types from two different manufacturers including Metl-Span CF-42 Mesa, Metl-Span CFR-42, Metl-Span LS-36, AWIP DM40, AWIP HR3 and AWIP SR2. The testing has been performed using the F-test setup, where connection restraint stiffness is determined by pulling on the free flange of a girt or purlin while measuring deflection (LaBoube 1986; Schafer et al. 2008; Gao and Moen 2012). The stiffness values derived from these tests can be used in a finite strip analysis in combination with the AISI Direct Strength Method to develop a calculation-based design approach as an alternative to full-scale system testing.

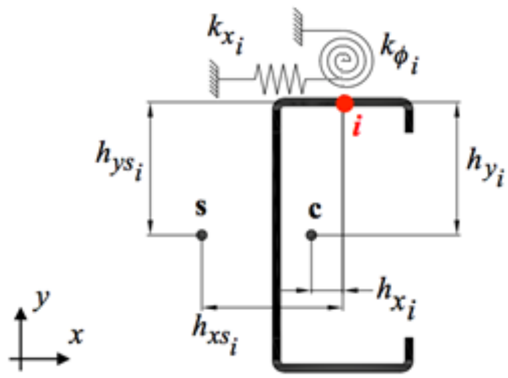

Figure 2. Model for IMP restraint of support member (Vieira 2011)

The following pages provide a description of the stiffness factors to be determined using the test results. Following that, a discussion of the analysis of the results is provided that includes parameter studies undertaken to evaluate the influence of overall panel thickness, support member cross-section type, and support member thickness. The stiffness values are summarized in a table intended for inclusion into future AISI specifications for design of cold-formed steel structural members supporting insulated metal panels.

2 Mechanical models for insulated metal panel restraint provided to girts and purlins

This chapter introduces the spring models for the attachment of the IMP to its support member that form the basis of the calculation-based design approach employing finite strip analysis of the cold-formed structural member and the AISI Direct Strength Method for determining capacities.

2.1 Connection rotational stiffness

Rotational restraint provided by the IMP-to-support connection is determined using the F-test apparatus shown in Figure 3. The connection rotational restraint stiffness with units of force*length/rad/length is calculated by using the applied moment and decomposed connection rotation with panel and web bending rotation imposed by the test procedure removed

$$k_\phi = \frac{M}{\theta_\phi} \qquad (1)$$

where $\theta_\phi = \theta - \theta_p - \theta_w$, $M=Qh_o$, and Q is a uniformly distributed load with units of force/length.

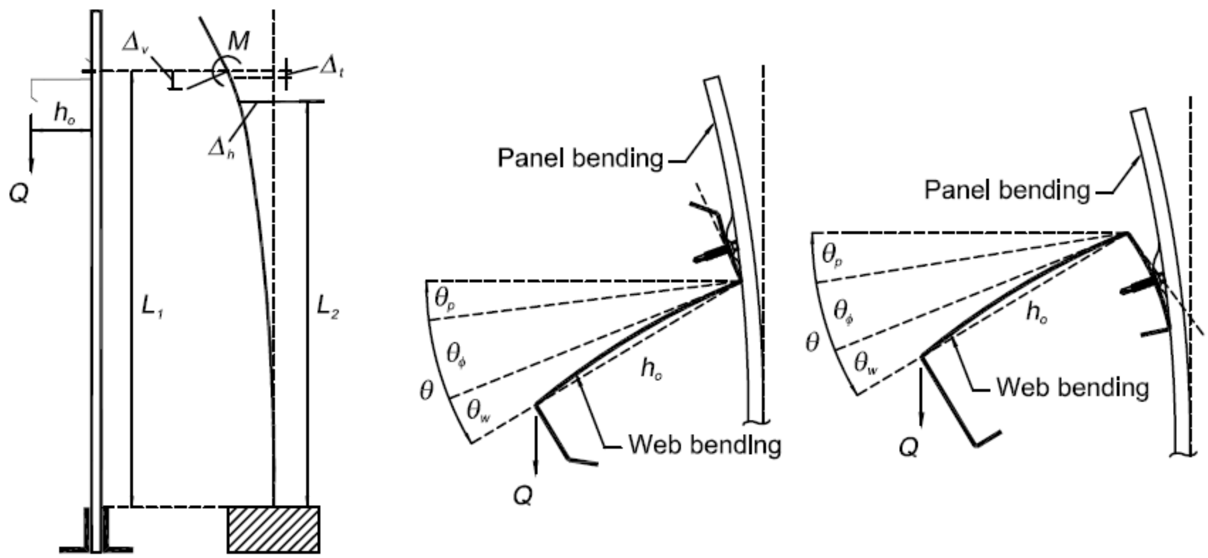

(a) (b)

Figure 3: (a) F-test model (b) Combination of rotation components

The distributed vertical load Q is applied and the vertical displacement Δ_v at the point of load application is measured. Panel horizontal displacement Δ_h is measured to calculate the rotation contribution at the connection from panel bending and the structural member (girt or purlin) vertical displacement Δ_t is measured to quantify the lateral bracing stiffness provided by the IMP. The Δ_v displacement is resolved into an equivalent rotation angle θ of the free flange/web juncture relative to the 'no-load' position and then decomposed into three rotational contributions – from panel cantilever bending θ_p, member web bending θ_w, and connection rotation θ_φ which total to approximately

$$\theta = \frac{\Delta_v}{h_0} \tag{2}$$

The panel rotation angle at the member connection due to cantilever bending θ_p is calculated as

$$\theta_p = \frac{2\Delta_h L_1}{L_2^2} \tag{3}$$

where L_1 is the distance from the fixed end of the panel to the member connection and L_2 is the location of the horizontal panel measurement, Δ_h.

The rotation of the free end of the member relative to the web-flange juncture at the panel attachment from member web bending is calculated from the deflection of an end-loaded cantilever as

$$\theta_w = \frac{\Delta_w}{h_o} = \frac{Qh_o^2}{3EI_w} \tag{4}$$

where EI_w is the member web flexural rigidity per unit length, E=29500 ksi, I_w=t^3/12, t is the support member thickness.

2.2 Connection translational stiffness

Translational restraint stiffness, k_x, with units of force/length/length along the member for a specified fastener spacing can be a significant factor in determining the lateral-torsional buckling capacity of girts and purlins, especially when the flange connected to the IMP is in compression where the lateral bracing capability of the panel connection can be utilized more effectively. This spring stiffness is calculated as

$$k_x = \frac{Q}{\Delta_t} \tag{5}$$

where Δ_t is the vertical deflection of the member shown in Figure 4 at the panel connection measured parallel to the flange load during the F test procedure.

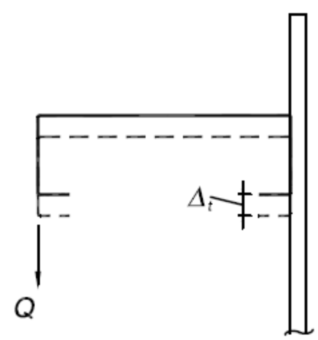

Figure 4: Translational restraint model

3 Experimental program

3.1 Testing strategy

F-tests were performed to measure the rotational and translational stiffness for typical metal building wall and roof systems constructed with insulated metal panels. A vertical load was applied to the unattached flange of Cee and Zee sections with IMPs attached to one flange. Linear variable differential transducers (LVDTs) and wire potentiometers were used to record the displacements corresponding to the loading, P, on the support member free flange shown in the Figures 5, 6, and 7 test schematics (Q is equal to P divided by the width of the panel specimen). LVDTs were used to measure the smaller displacements Δ_h and Δ_t, and wire potentiometers were used to capture the larger Δ_v displacements.

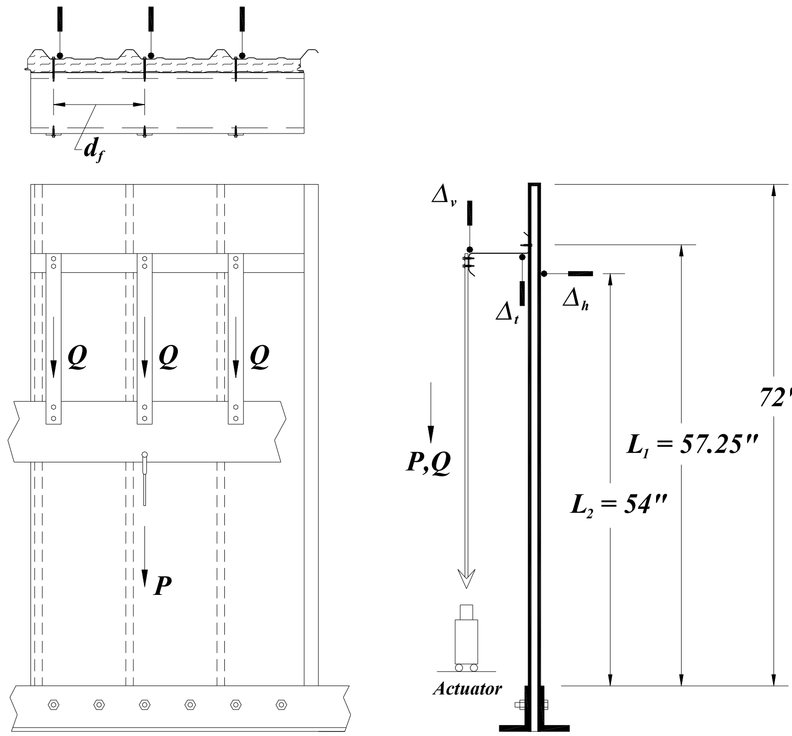

Figure 5: Through-Fastened IMP Wall Panel Test Setup

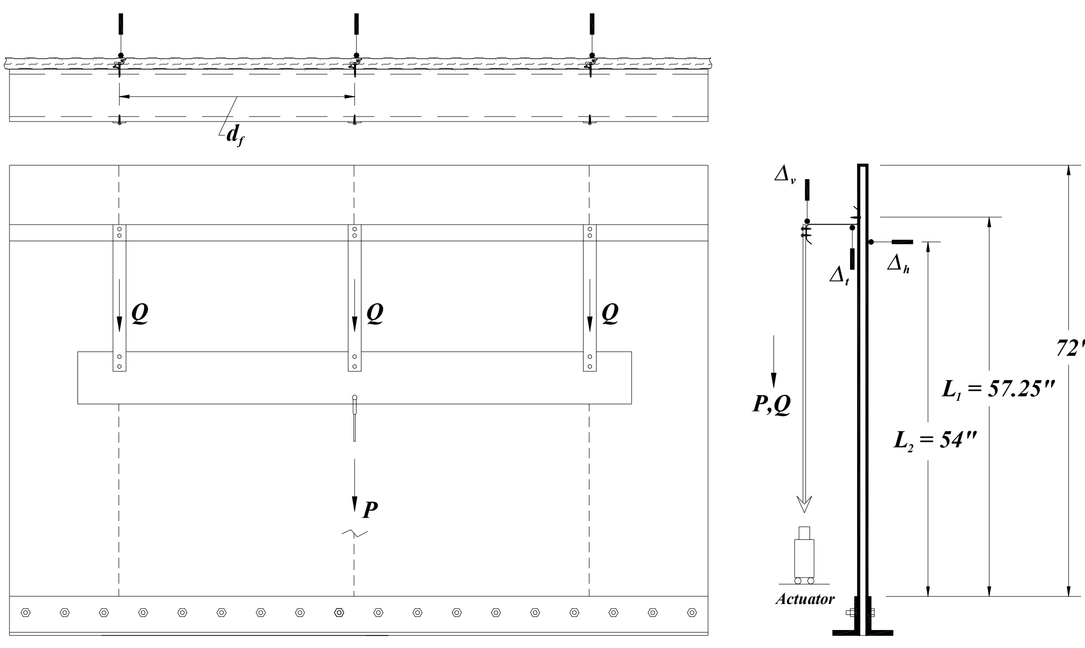

Figure 6: Concealed-Fastener IMP Wall Panel Test Setup

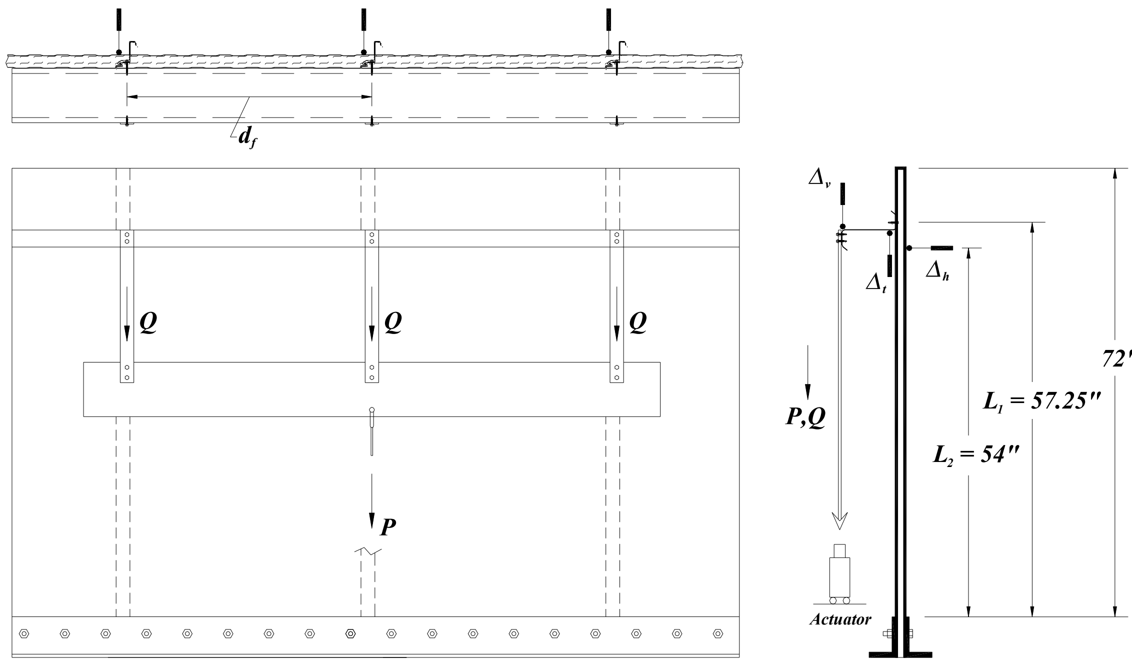

Figure 7: Concealed-Fastener IMP Roof Panel Test Setup

3.2 Test matrix

Representative insulated metal panels from two different manufacturers were evaluated. The experimental variables considered were panel type (CF-42, CFR-42, LS-36, DM40, HR3 and SR2), total panel thickness (2 in. and 4 in.), and cold-formed steel structural member cross-section type and depth (C8, C12, Z8, and Z12). Of the different panel types, CF-42 and DM40 were of the concealed-fastener wall type, CFR-42 and SR2 were of the concealed-fastener standing-seam roof type, and LS-36 and HR3 were of the through-fastened panel type. CF-42, CFR-42, and LS-36 were composed of a polyurethane-based foam while DM40, HR3, and SR2 were composed of a polyisocyanurate-based foam. No attempt was made to distinguish differences in response between the two IMP foam types in these tests. A list of the tests conducted along with the different variables chosen for each test is shown in Table 1.

Table 1: Testing Matrix

Panel Type	Test Number	Panel Thickness	Cold-formed Member	Member Type
CF-42 Mesa - concealed-fastener wall panel [42"]	A1	2"	C8-12 x 96"	Cee
	A2	2"	C8-12 x 96"	Cee
	A3	2"	C8-12 x 96"	Cee
	B1	4"	C8-12 x 96"	Cee
	B2	4"	C8-12 x 96"	Cee
	B3	4"	C8-12 x 96"	Cee
	C1	2"	Z8-12 x 96"	Zee
	C2	2"	Z8-12 x 96"	Zee
	C3	2"	Z8-12 x 96"	Zee
	D1	4"	Z8-12 x 96"	Zee
	D2	4"	Z8-12 x 96"	Zee
	D3	4"	Z8-12 x 96"	Zee
	E1	2"	Z8-16 x 96"	Zee
	E2	2"	Z8-16 x 96"	Zee
	E3	2"	Z8-16 x 96"	Zee
CFR-42 - Standing seam concealed-fastener roof panel [42"]	F1	2"	Z8-12 x 96"	Zee
	F2	2"	Z8-12 x 96"	Zee
	F3	2"	Z8-12 x 96"	Zee
	G1	4"	Z8-12 x 96"	Zee
	G2	4"	Z8-12 x 96"	Zee
	G3	4"	Z8-12 x 96"	Zee
LS-36 - Through-fastened panel - wall attachment [36"]	H1	2"	Z8-12 x 36"	Zee
	H2	2"	Z8-12 x 36"	Zee
	H3	2"	Z8-12 x 36"	Zee
	I1	4"	Z8-12 x 36"	Zee
	I2	4"	Z8-12 x 36"	Zee
	I3	4"	Z8-12 x 36"	Zee
DM40 - Concealed-fastener wall panel [40"]	J1	2"	Z8-16 x 92"	Zee
	J2	2"	Z8-16 x 92"	Zee
	J3	2"	Z8-16 x 92"	Zee
	K1	4"	Z8-16 x 92"	Zee
	K2	4"	Z8-16 x 92"	Zee
	K3	4"	Z8-16 x 92"	Zee
HR3 - Through-fastened roof panel [40"]	L1	4"	Z8-12 x 36"	Zee
	L2	4"	Z8-12 x 36"	Zee
	L3	4"	Z8-12 x 36"	Zee
	M1	4"	Z12-12 x 36"	Zee
	M2	4"	Z12-12 x 36"	Zee
	M3	4"	Z12-12 x 36"	Zee
SR2 - Standing seam concealed-fastener roof panel [40"]	N1	4"	Z12-12 x 92"	Zee
	N2	4"	Z12-12 x 92"	Zee
	N3	4"	Z12-12 x 92"	Zee

3.3 Test specimen dimensions

3.3.1 Cold-formed structural member cross-section dimensions

The nominal dimensions of the cold-formed Cee and Zee sections used in this study are provided in Figure 8.

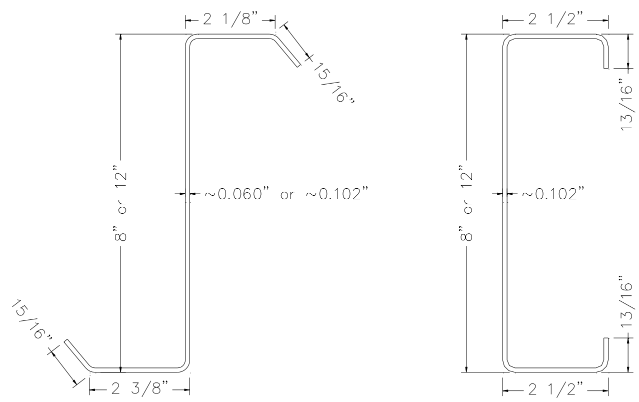

Figure 8: Cee and Zee cross-section dimensions

3.3.2 Cold-formed structural member base metal thickness

The cold-formed Cee and Zee structural members tested were designated as C8-12, Z8-12, Z8-16 and Z12-12 where the first number denotes out-to-out web height in inches (8 or 12) and the number after the dash designates gauge thickness (12 or 16). The bare steel base metal thicknesses were measured with a micrometer prior to testing for sample members formed from the same coil and are shown in Table 2.

Table 2: Structural member base metal thickness

Cold-formed Member	Test Number	Base Metal Thickness	Mean Thickness
C8-12	A1 A2 A3	0.102" 0.103" 0.102"	0.102"
Z8-12	C1 C2 C3	0.102" 0.102" 0.102"	0.102"
Z8-16	E1 E2 E3	0.059" 0.060" 0.061"	0.060"
Z12-12	M1 M2 M3	0.104" 0.103" 0.103"	0.103"

3.3.3 *Insulated metal panel dimensions*

The IMP cross-sections tested are shown in Figure 9. Each panel type was tested at 2 in. and 4 in. thickness. Overall panel width varied by panel type.

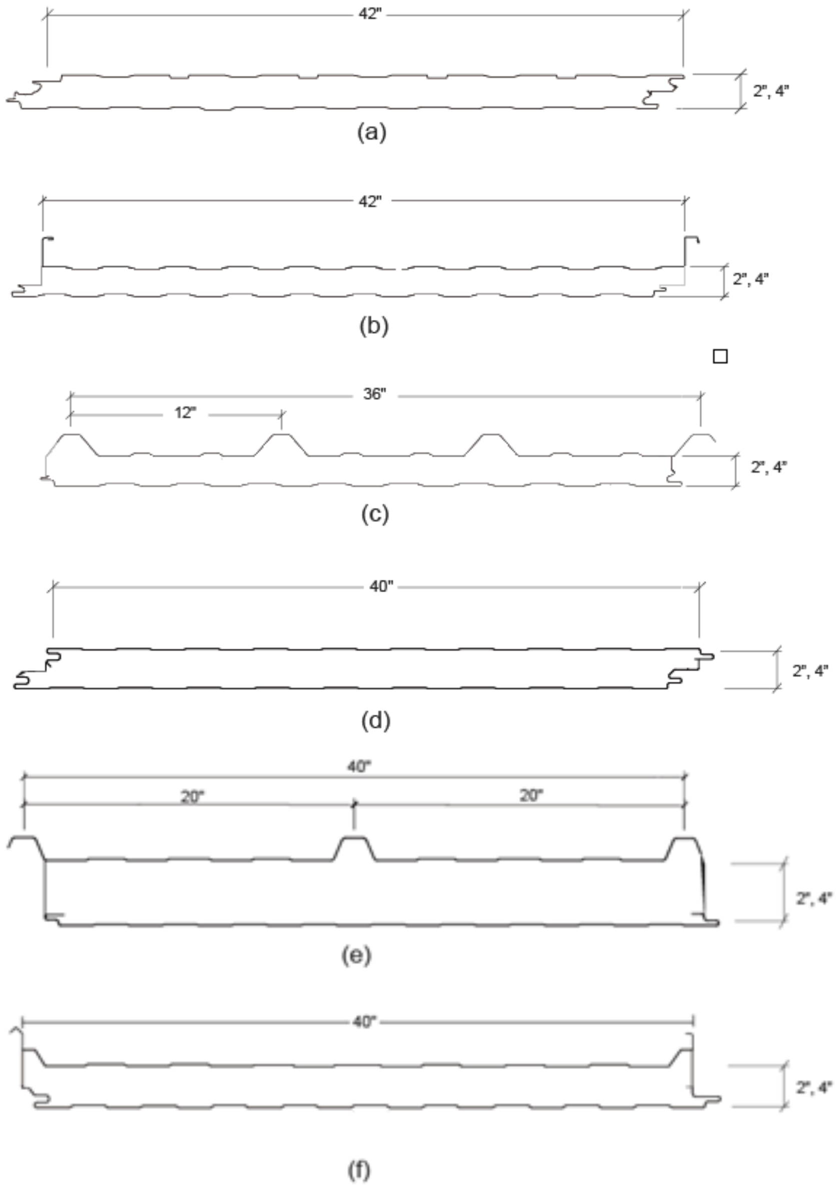

Figure 9: Panel cross-sections - (a) CF-42 wall panel; (b) CFR-42 roof panel; (c) LS-36 roof and wall panel; (d) DM40 wall panel; (e) HR3 roof panel; (f) SR2 roof panel

3.3.4 *Connection type*

Three different panel-to-structural member connection types were evaluated – wall concealed fastener, through-fastened, and standing seam roof concealed fastener connections. Drawings and test photos are shown in Figure 10.

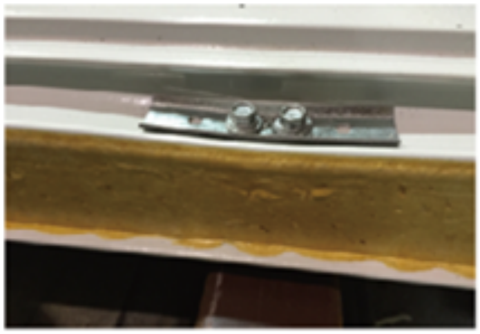

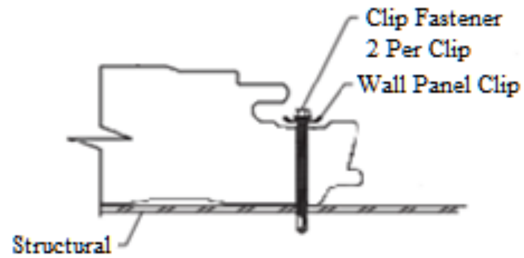
Clip Fastener
2 Per Clip
Wall Panel Clip
Structural

(a)

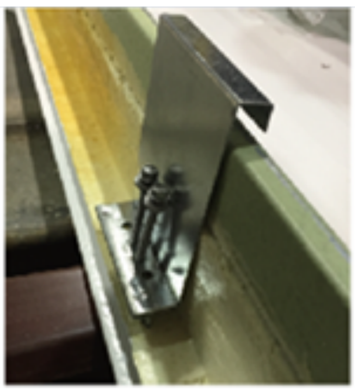

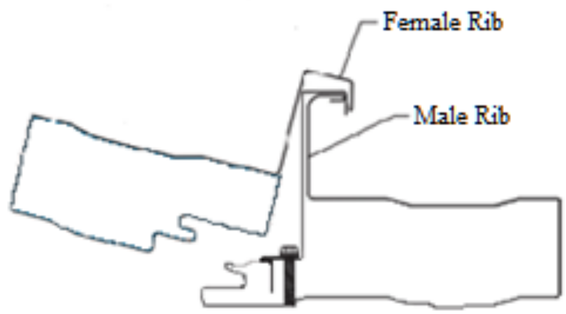
Female Rib
Male Rib

(b)

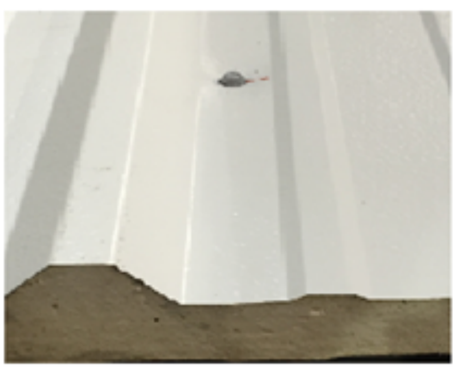

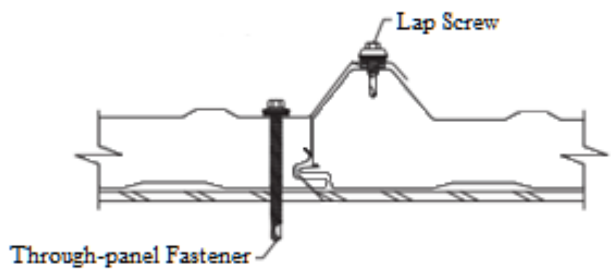
Lap Screw
Through-panel Fastener

(c)

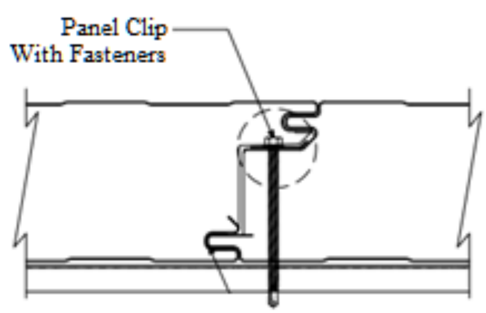
Panel Clip
With Fasteners

(d)

(e)

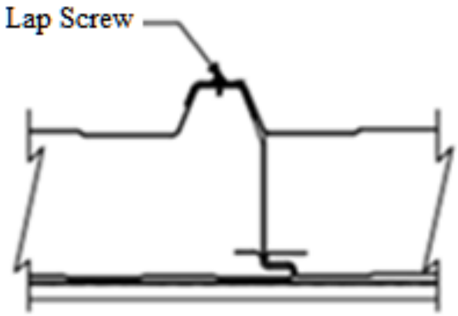

(f)

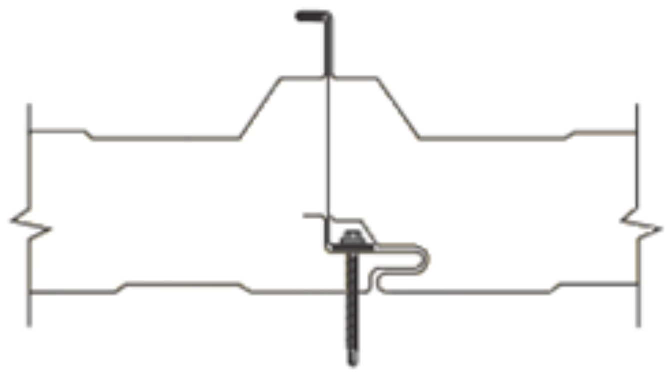

Figure 10: Panel types tested - (a) CF-42 wall panel; (b) CFR-42 roof panel; (c) LS-36 roof panel; (d) DM40 wall panel; € HR3 roof panel; (f) SR2 roof panel

3.3.5 Screw fastener details

1/4” x 2” self-drilling screws (SDS) were used to attach the CFR-42 and SR2 panels through the clips designed for each panel that are concealed in the side joint. 1/4" x 3” SDS were used to attach the 2” CF-42 and 2” DM40 panels through their respective side joint clips. The same 1/4" x 3” SDS were used to attach the 2” through-fastened LS-36 and HR3 panels adjacent to the high rib of the exterior sheet. 1/4" x 5” SDS were used to attach the 4” CF-42, DM40, LS-36, and HR3 panels in the same manner as described for their 2” versions. Typical panel attachment screws are shown in Figure 11.

Figure 11: Typical panel attachment self-drilling screws

Approximate screw locations in the structural member flange are provided in Figure 12 below.

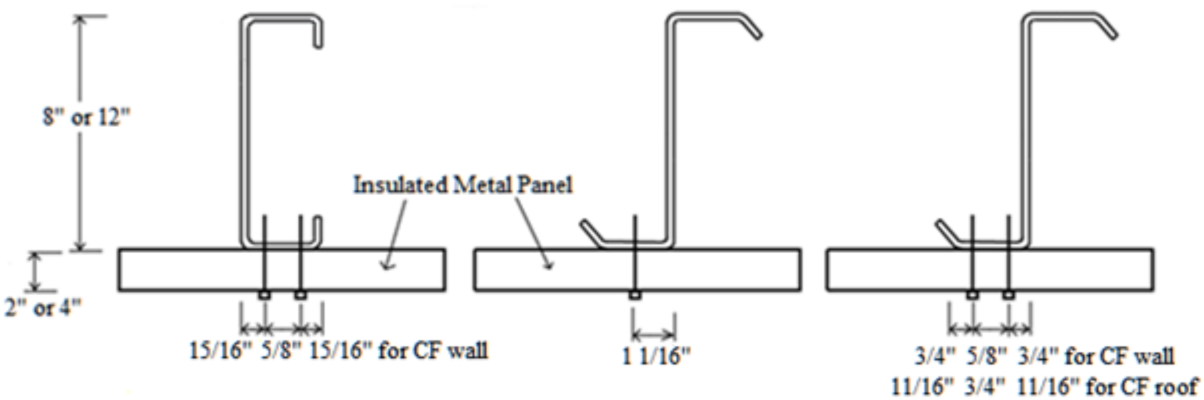

Figure 12: (a) Concealed-fastener wall panel attachment to Cee; (b) Through-fastened panel attachment to Zee (c) Concealed-fastener roof and wall panel attachment to Zee

3.4 Test setup

Each assembly was a combination of panels and Cee or Zee specimen. Panels were connected using their specified fasteners at the panel edges to form a 126 in × 72 in (CF-42, CFR-42), 120 in. × 72 in. (DM40, SR2), 36 in. × 72 in. (LS36), or 40 in. × 72 in. (HR3) assembly. The base of each panel was clamped between 8 in. × 6 in. × 5/16 in. steel angles with pre-drilled holes every 6 in. and through-bolted with 5/8" structural bolts. The experimental setup is shown in Figure 13.

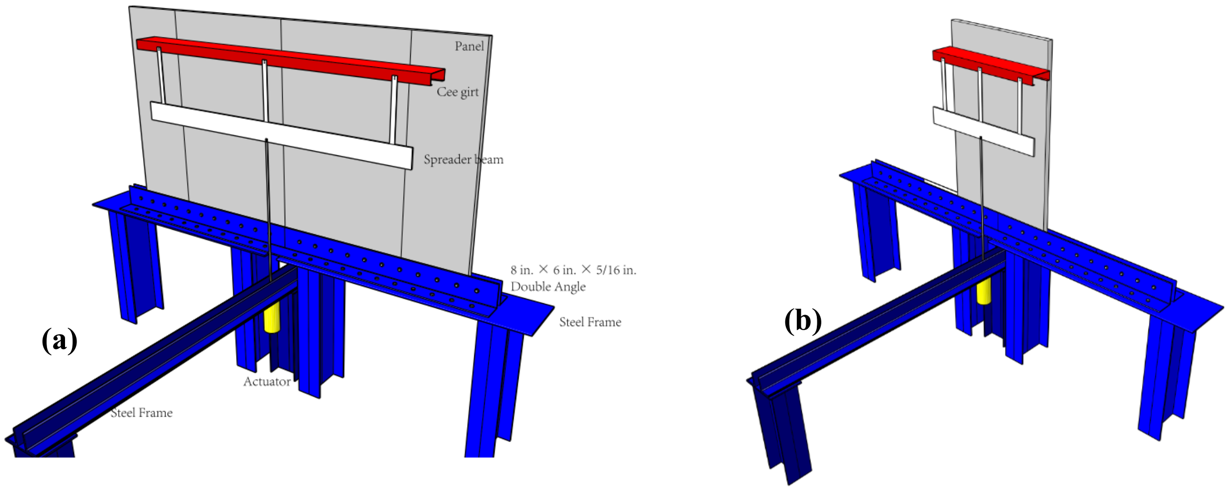

Figure 13. Test setup for (a) concealed fastener roof and wall panels; and (b) through fastened panels

3.5 Instrumentation

A set of two LVDTs with an accuracy of +/- 0.01 in. were used to measure horizontal displacement of the panels (Δ_h in Figure 3) and relative displacement between panels and girts (Δ_t in Figure 4). Wire potentiometers (WP) were used to measure the total vertical displacement of the deflected girts, Δ_v as shown in Figure 3. Also, a tension load cell (accuracy of +/- 0.01 in.), was connected between the spreader beam and pull jack to measure the total applied load, P.

3.6 Specimen preparation and installation

The concealed-fastener wall and roof test assemblies using CF-42, DM40, CFR-42, and SR2 were formed with two full panel widths sandwiched between half-width panel sections at each side so that two concealed connections in the side joints were tested. In addition the half-width panels were attached at the exterior edges with a through-fastened connection to the cold-formed structural member. The through-fastened test assemblies using LS-36 and HR3 panels were formed with only one panel and were attached through the flat of the panel at 12” o.c.

3.7 Test procedure

Before recording data, an overhead crane was used to support the initial weight of the spreader beam. Immediately after data recording began, the crane support of the spreader beam was slowly released and additional load was applied by a pull jack with a hand pump. Although the loading rate could not be controlled precisely, the rate was estimated to be approximately 5 lbs/sec. Load and deflection data were collected until connection degradation led to overly large deformations of the specimen.

3.8 Material properties

The steel yield stress for each cold-formed structural member was determined with tensile coupon tests according to ASTM E8 / E8M, “Standard Test Methods for Tension Testing of Metallic Materials” (ASTM 2015). Coupons were taken from of the top flange, web, and bottom flange elements of each size of Cee and Zee tested. The surface paint was removed with steel wool and acetone before measuring the base metal thickness. The yield stress for each specimen type is summarized in Table 3.

Table 3: Cold-formed structural member yield stress from tensile coupons

Cold-formed Member	Sample Name and Location	Yield Stress (ksi)	Cold-formed Member	Sample Name and Location	Yield Stress (ksi)
C8-12	C8-12-1t	68	Z8-16	Z8-16-1t	68
	C8-12-1w	69		Z8-16-1w	66
	C8-12-1b	69		Z8-16-1b	64
	C8-12-2t	68		Z8-16-2t	66
	C8-12-2w	70		Z8-16-2w	65
	C8-12-2b	69		Z8-16-2b	63
	C8-12-3t	64		Z8-16-3t	67
	C8-12-3w	67		Z8-16-3w	67
	C8-12-3b	68		Z8-16-3b	65
Z8-12	Z8-12-1t	68	Z12-12	Z12-12-1t	65
	Z8-12-1w	70		Z12-12-1w	65
	Z8-12-1b	65		Z12-12-1b	67
	Z8-12-2t	69		Z12-12-2t	66
	Z8-12-2w	68		Z12-12-2w	66
	Z8-12-2b	65		Z12-12-2b	68
	Z8-12-3t	69		Z12-12-3t	66
	Z8-12-3w	70		Z12-12-3w	67
	Z8-12-3b	65		Z12-12-3b	68

4 Experimental results

4.1 General observations

The typical behavior seen during the tests was for a small gap to open between the structural member top edge and the panel due to localized deformation at the connection followed by fastener pullout from the structural member. Plastic flexural deformation was observed both in the screws and the concealed-fastener wall connection plates as shown in Figure 14. A typical load-deformation response curve is shown in Figure 15, with nonlinearity prominent up to fastener pull-out caused by local panel deformation from bearing of the compression side of the attached cold-formed flange and panel foam compression under the screw connection.

(a) (b)

Figure 14: (a) local connection deformation; (b) deformed screws and plates after testing

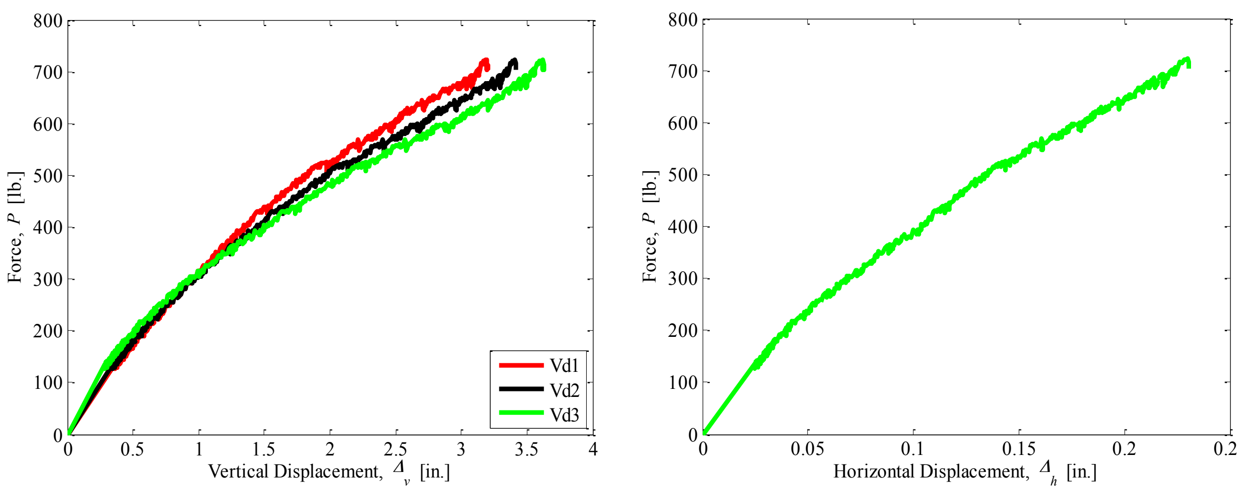

Figure 15: Total Load, P, vs. displacement (Δ_v (left) and Δ_h (right) from test B2)

4.2 Rotational and translational spring stiffness

Restraint provided by the IMPs to the tested purlins is summarized in Table 4. The translational stiffness k_x is calculated by taking the slope of the secant in the P-Δ_h plot between the load-deflection reading just after the spreader beam weight is applied and the P_2 load that creates a screw pullout force of one-half of the pullout strength calculated from the 2012 AISI S100 specification. Note that for the 4” HR3 tests, the test load never reached that screw tension level, so the screw pullover strength of the 26 ga exterior sheet of the IMP was used instead. The differences in panel encapsulation for pullout capacity between a metal-to-metal connection and the connection used for IMPs where an intermediate layer of more flexible foam exists between the metal layers will cause the S100 equations to overestimate the pullover capacity of the actual IMP connection. However, the end result will yield a lower and more conservative translational stiffness value than what might be achieved with a better estimate of true pullover capacity. Utilized in this manner, use of the AISI equations was considered acceptable. The rotational stiffness k_ϕ was determined as the ratio of the imposed moment at the P_2 load and the connection rotation determined at load P_2. The spring stiffnesses shown in Table 4 can be applied in a finite strip model to simulate system effects in an IMP wall or roof system when determining girt and purlin strength using the AISI Direct Strength Method.

Table 4: Insulated metal panel restraint stiffness provided to a girt or purlin

Panel Type	Test Number	k_ϕ (lb-in./rad/in.)			k_x (lb/in./in.)		
		Test	Mean	COV	Test	Mean	COV
CF-42 Mesa - concealed-fastener wall panel [42"]	A1	286	286	0.06	N/A	N/A	N/A
	A2	264			N/A		
	A3	307			N/A		
	B1	N/A	234	0.08	108	74	0.32
	B2	215			58		
	B3	253			58		
	C1	295	296	0.11	79	78	0.01
	C2	339			77		
	C3	255			N/A		
	D1	318	312	0.08	50	52	0.02
	D2	338			N/A		
	D3	279			53		
	E1	217	191	0.13	43	43	0.01
	E2	166			44		
	E3	N/A			N/A		
CFR-42 - Standing seam concealed-fastener roof panel [42"]	F1	404	404	N/A	84	84	N/A
	F2	N/A			N/A		
	F3	N/A			N/A		
	G1	356	354	0.11	60	61	0.03
	G2	307			63		
	G3	399			59		
LS-36 - Through-fastened panel - wall attachment [36"]	H1	N/A	N/A	N/A	28	30	0.04
	H2	N/A			31		
	H3	N/A			31		
	I1	217	245	0.09	27	31	0.09
	I2	269			34		
	I3	250			31		
DM40 - Concealed-fastener wall panel [40"]	J1	167	194	0.11	43	41	0.04
	J2	221			40		
	J3	194			40		
	K1	218	206	0.20	35	32	0.12
	K2	249			34		
	K3	151			26		
HR3 - Through-fastened roof panel [40"]	L1	162	171	0.07	24	22	0.08
	L2	165			20		
	L3	187			21		
	M1	230	205	0.10	17	16	0.09
	M2	203			16		
	M3	180			14		
SR2 - Standing seam concealed-fastener roof panel [40"]	N1	307	294	0.05	30	30	0.02
	N2	280			31		
	N3	N/A			N/A		

4.3 Influence of panel thickness on rotational restraint

The connection responses for the CF-42 concealed-fastener wall panel at 2 in. and 4 in. depths (tests A1, B3, C1 and D1) are plotted in Figure 16 for both cees and zees. The similarity of response characteristics shows that the IMP thickness has a minimal influence on rotational stiffness. The IMP metal skin is braced by the connection plate and underlying insulation as the fastener pulls out, and this support provides similar stiffness regardless of the overall panel thickness.

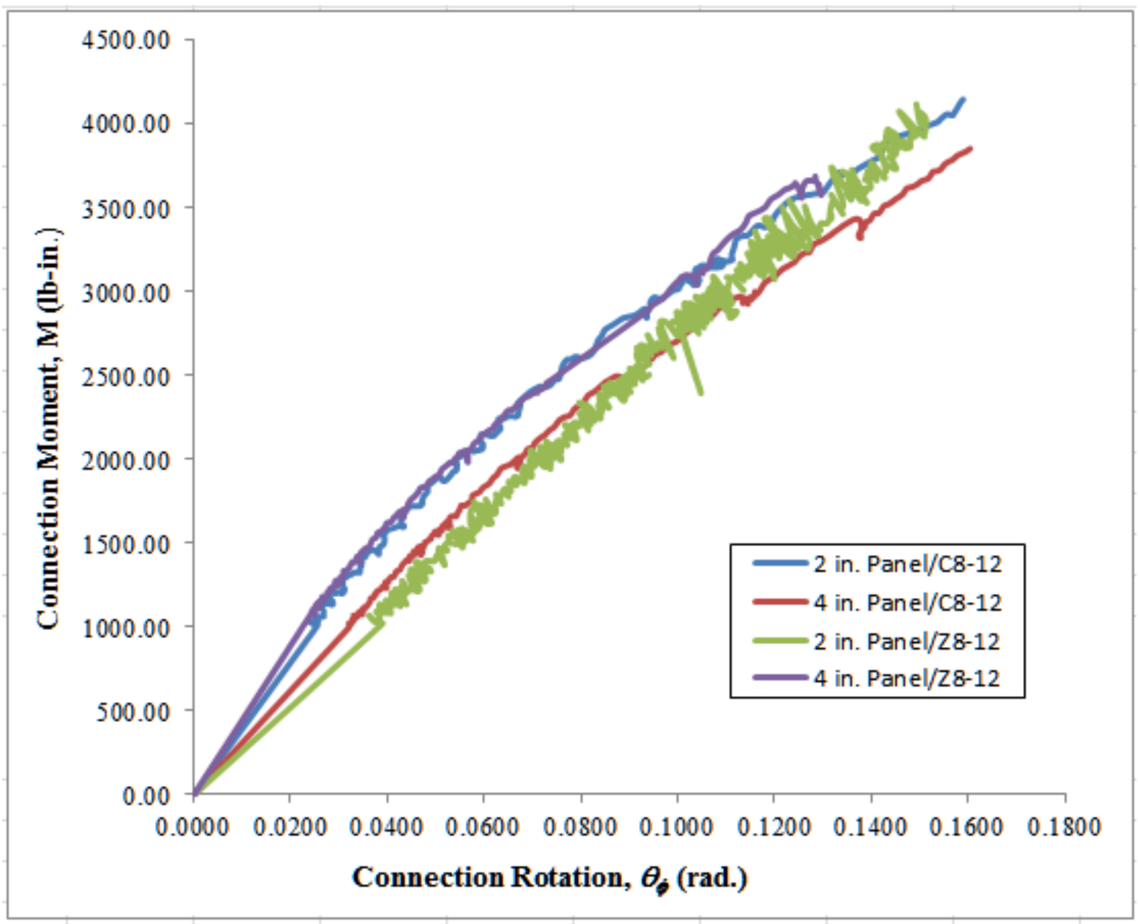

Figure 16: Comparison of moment-rotation curves for 2" and 4" thick IMPs (Tests A1, B3, C1 and D1 shown)

4.4 Influence of cold-formed member cross-section shape on rotational restraint

IMP rotational restraint stiffness provided to both a Cee and Zee section of the same base metal thickness is compared in Figure 17 for the same CF-42 concealed-fastener wall panel (Tests A1 and C1). The rotational restraint in the Zee section is approximately 9.3% higher than the Cee at ultimate level deflections, but shows almost identical restraint stiffness at allowable stress levels, estimated here to be approximately 50% of ultimate deflections. This shows that the difference in restraint stiffness for Cee and Zee cold-formed support member cross-section shapes is negligible.

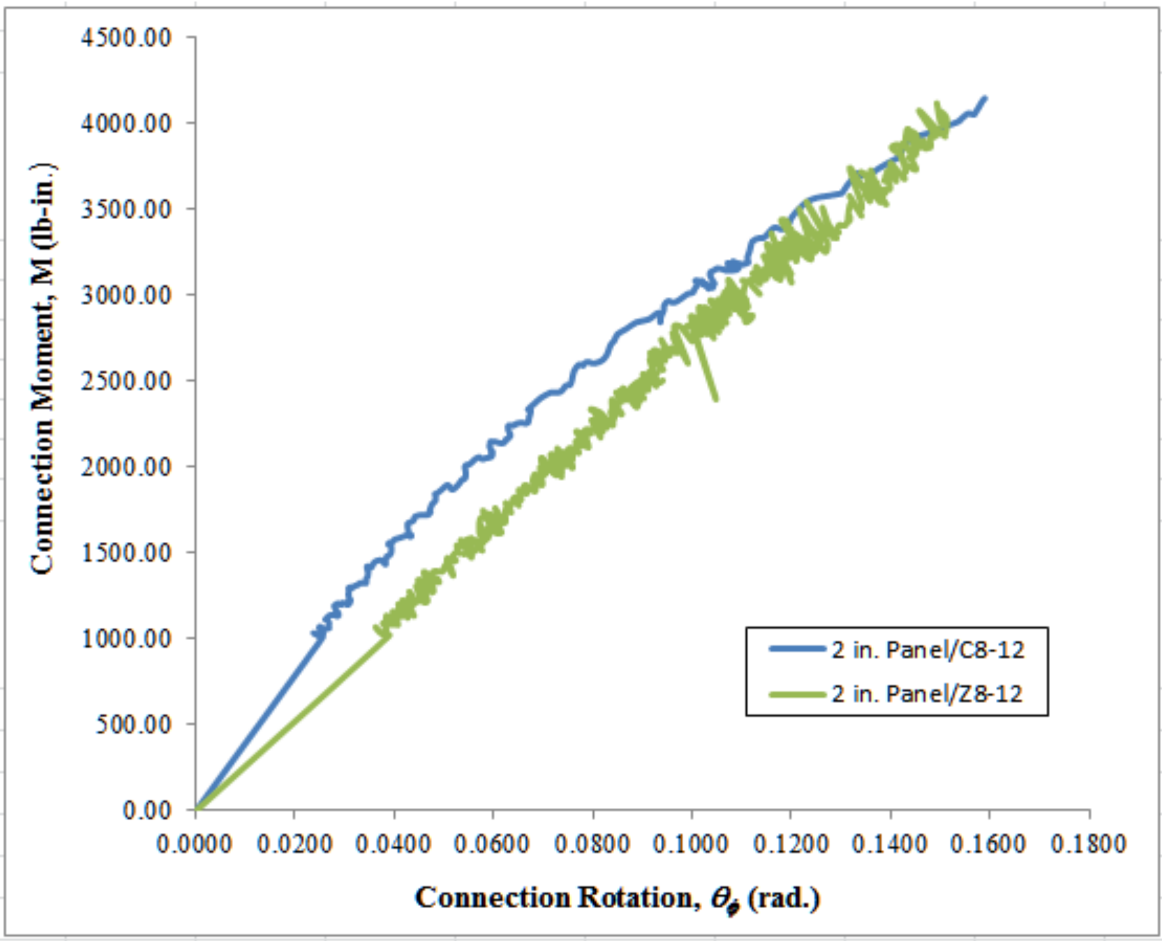

Figure 17: Comparison of moment-rotation curves for Cees and Zees (Tests A1 and C1 shown**)**

4.5 Influence of cold-formed member thickness on rotational restraint

Connection rotational restraint is known to be strongly influenced by the thickness of the cold-formed structural member being restrained. Local bending in the attached flange reduces rotational restraint and this is confirmed in the comparison of the results of tests C3 and E2 performed on the CF-42 concealed-fastener wall IMP over 12 ga (0.102”) and 16 ga. (0.060”) Zees, shown in Figure 18. The rotational stiffness is 166 lb.-in/rad/in for the 16 gauge specimen compared to 255 lb.-in/rad/in for the 12 gauge specimen, a 54% increase in stiffness with increasing support member thickness.

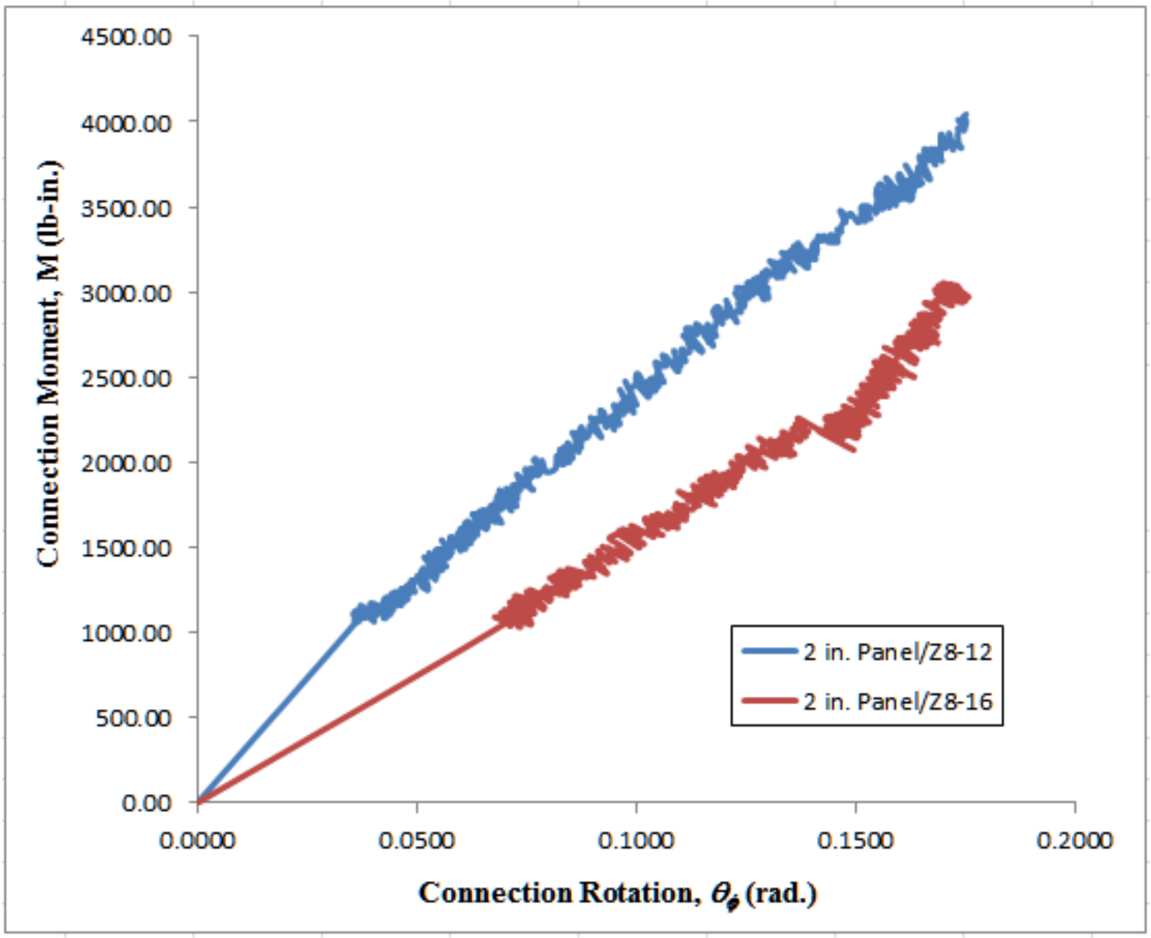

Figure 18: Comparison of moment-rotation curves for 12 ga. and 16 ga. structural members (tests C3 and E2 shown)

4.6 Influence of panel attachment type on rotational restraint

Rotational restraint stiffness varies based on the type of panel and attachment employed. Concealed-fastener standing seam roof IMP panel attachment showed the highest rotational stiffness, while the through-fastened IMP panel attachment provided the least rotational stiffness. In comparing tests D1 (concealed-fastener wall CF-42), G1 (concealed-fastener standing seam roof CFR-42) and I3 (through-fastened LS-36), there is a 27% increase (Fig. 19) for rotational stiffness in concealed-fastener wall panel attachment over through-fastened panel attachment.
There is an additional 14% increase in concealed-fastener standing seam roof panel attachment over concealed-fastener wall panel attachment. Note that while the CF Roof and CF Wall graphs appear similar in the individual test graphs shown in the chart below, the average of the rotational stiffnesses for all tests within the groups do show the increases described above.

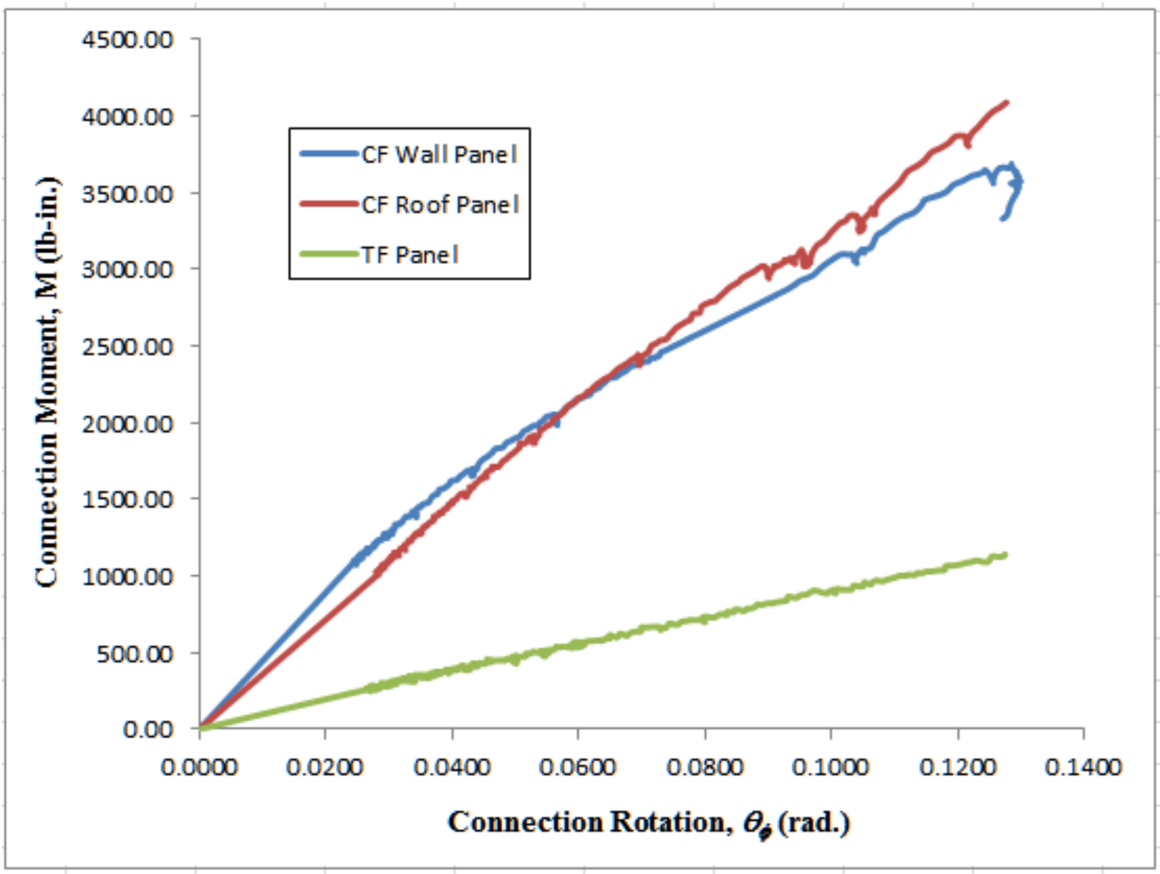

Figure 19: Rotational stiffness comparison of concealed-fastener wall, concealed-fastener standing seam roof, and through-fastened IMP attachment; D1 (blue), G1 (red) and I3 (green)

5 Conclusions

Experiments on insulated metal panels were conducted to quantify the influence of different connection types, cross-section types, and panel thickness. Rotational and translational spring stiffnesses for IMPs were obtained and summarized for use in future analysis-based design code provisions. Rotational stiffness is sensitive to the support member thickness with the thicker cold-formed member developing larger rotational stiffness. Rotational stiffness is minimally influenced by IMP panel thickness and support member cross-section shape. Concealed-fastener standing seam roof connections provided the highest rotational restraint for the the panels tested. The results of the research yielded spring stiffness values that can be used in conjunction with a finite strip analysis to predict system capabilities greater than those determined by treating each component in isolation, and this increase in strength can be achieved without performing more in-depth and costly full-scale system experiments.

References

Gao, T., Moen, C.D. (2012). "Predicting Rotational Restraint Provided to Wall Girts and Roof Purlins by Through-Fastened Metal Panels." *Thin-Walled Structures*, 61, 145-153.

LaBoube, R.A. (1986). "Roof Panel to Purlin Connections: Rotational Restraint Factor." *Proceedings of the IABSE Colloquium on Thin-Walled Metal Structures in Building*s, Stockholm, Sweden.

Fisher, J.M. (1996). Uplift capacity of simple span Cee and Zee members with through-fastened roof panels. *Final report: MBMA 95-01*. Cleveland, Ohio: Metal Building Manufacturers Association.

ASTM E8 / E8M-15 (2015). Standard Test Methods for Tension Testing of Metallic Materials, ASTM International, West Conshohocken, PA, 2015.

AISI-S100 (2012). North American Specification For The Design Of Cold-Formed Steel Structural Members. Washington, DC: American Iron and Steel Institute; 2012.

Gao T., Moen C.D. (2012). Direct strength flexural capacity prediction of through-fastened cold-formed steel roof purlins and wall girt systems wind uplift or suction. *Proceedings Of The Twenty-first International Specialty Conference On Cold-Formed Steel Structures*. St. Louis, Missouri

Schafer, B.W., Sangree, R. H., Guan, Y. (2008). "Rotational Restraint of Distortional Buckling in Cold-Formed Steel Framing Systems." *Proc., Fifth International Conference on Thin-Walled Structures*, Brisbane, Australia.

Vieira Jr., L.C.M. (2011). Behavior and design of cold-formed steel stud walls under axial compression, Department of Civil Engineering, *Ph.D. Dissertation*, Johns Hopkins University.

Appendix A - Load vs. Vertical unfastened flange deflection, Δ_v

The following charts show the results for cold-formed member unattached flange vertical deflection measured behavior with the total load P (applied tension load plus spreader bar weight). Results of like tests using identical cold-formed member depths and thicknesses, panel types, and overall panel thicknesses are shown on the same chart. The Table 1 test matrix is reprinted here for clarity and convenience.

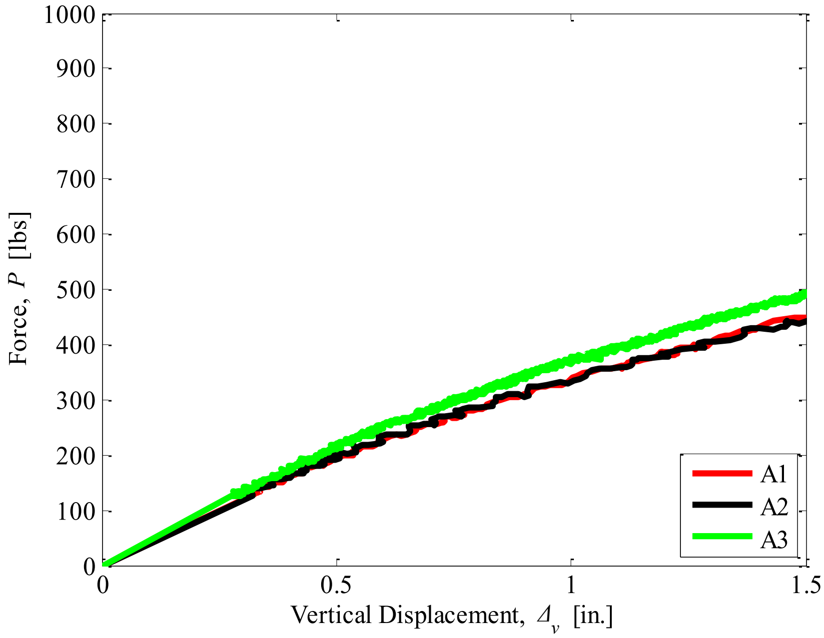

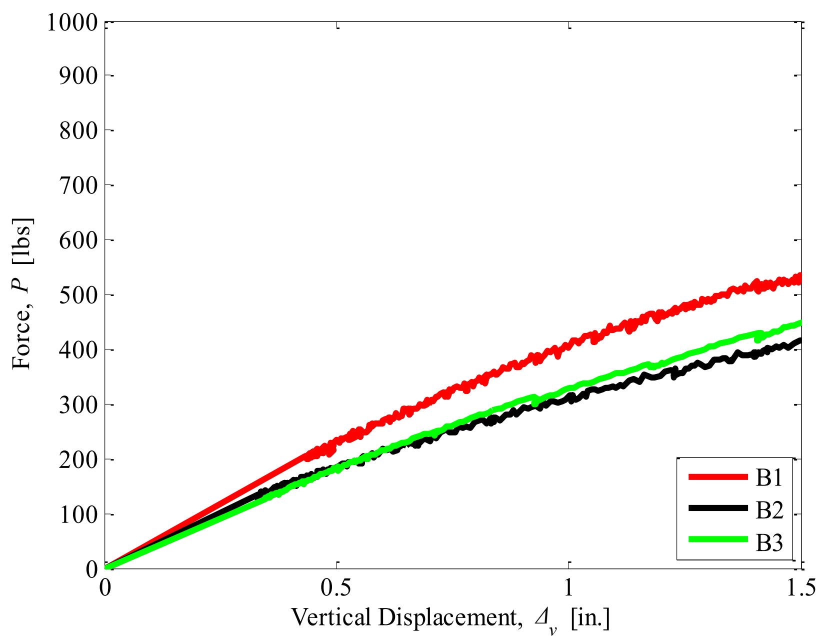

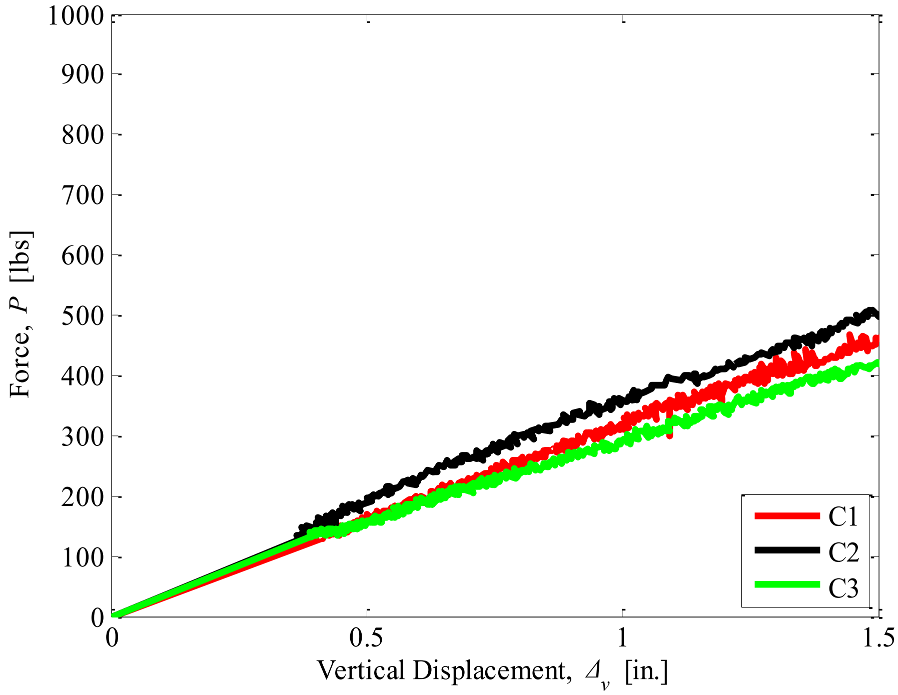

1000
900
800
700
600
500
400
300
200
100
0
Force, P [lbs]
0
0.5
1
1.5
Vertical Displacement, Δ_v [in.]
C1
C2
C3

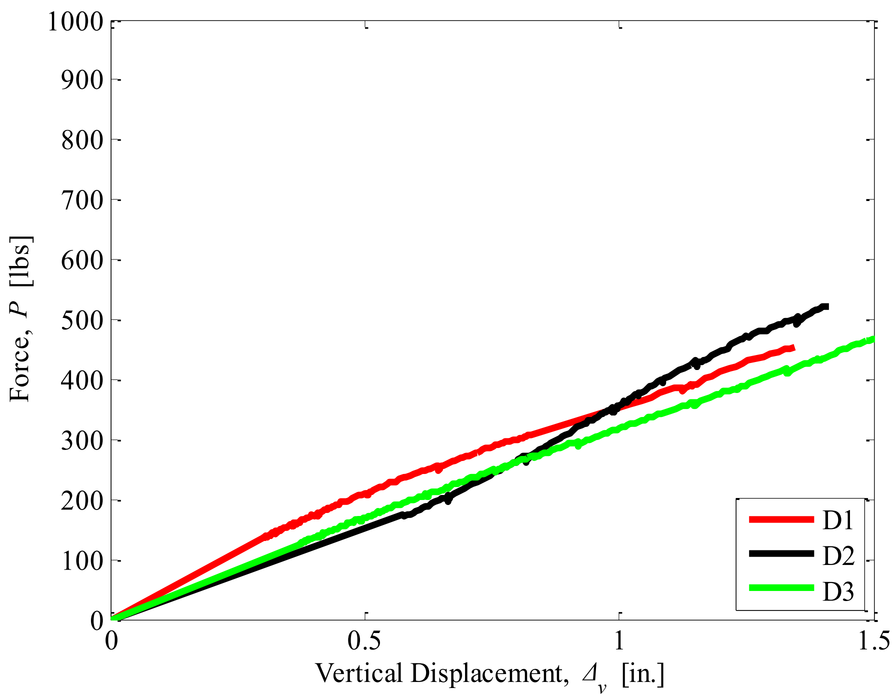

1000
900
800
700
600
500
400
300
200
100
0
Force, P [lbs]
0
0.5
1
1.5
Vertical Displacement, Δ_v [in.]
D1
D2
D3

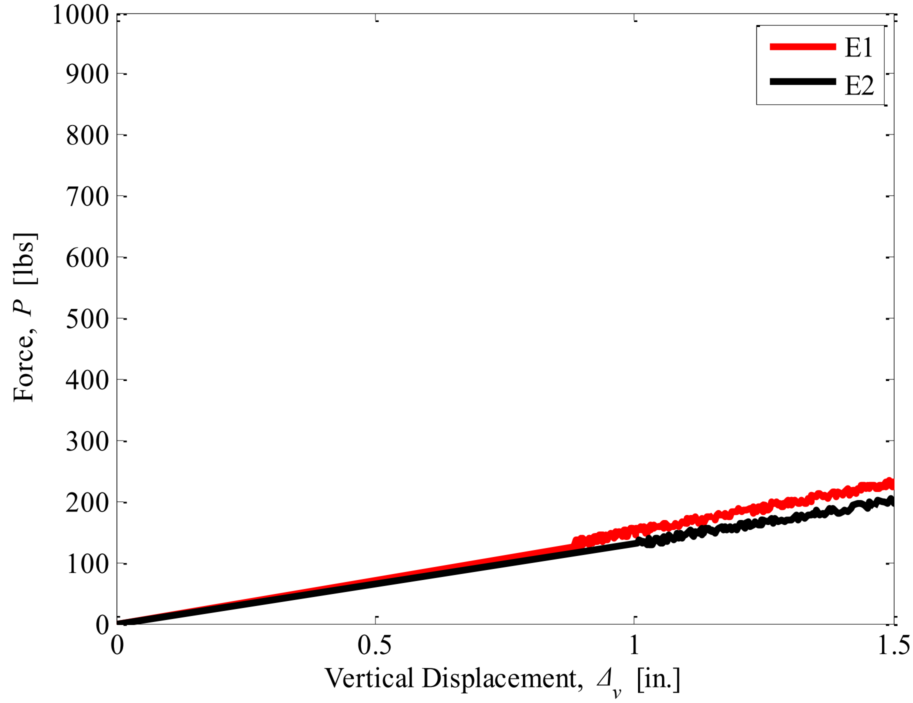

E1
E2
Force, P [lbs]
Vertical Displacement, Δv [in.]
0
100
200
300
400
500
600
700
800
900
1000
0
0.5
1
1.5

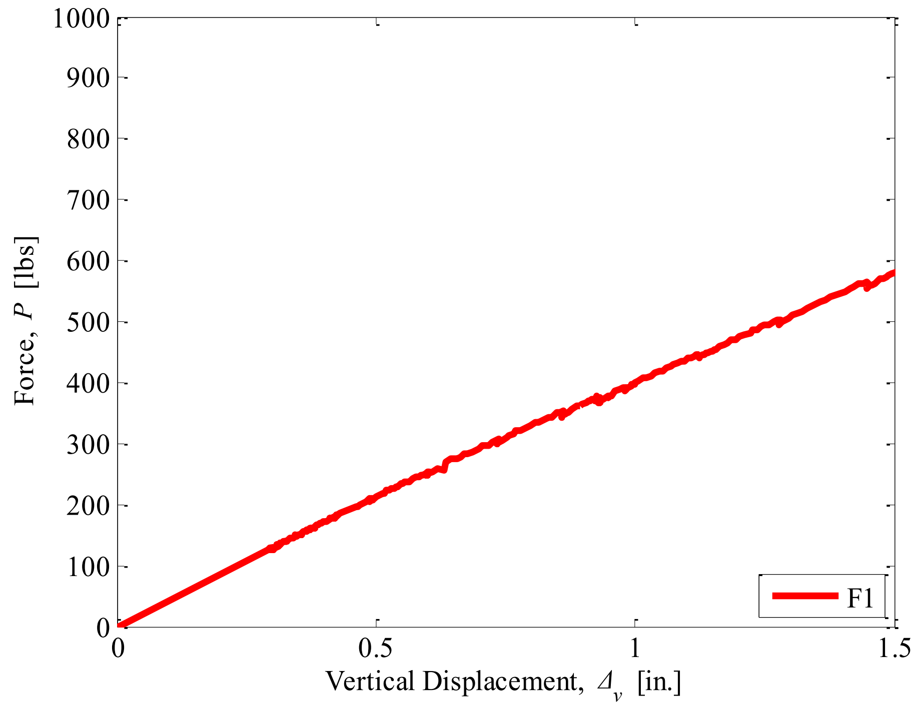

F1
Force, P [lbs]
Vertical Displacement, Δv [in.]
0
100
200
300
400
500
600
700
800
900
1000
0
0.5
1
1.5

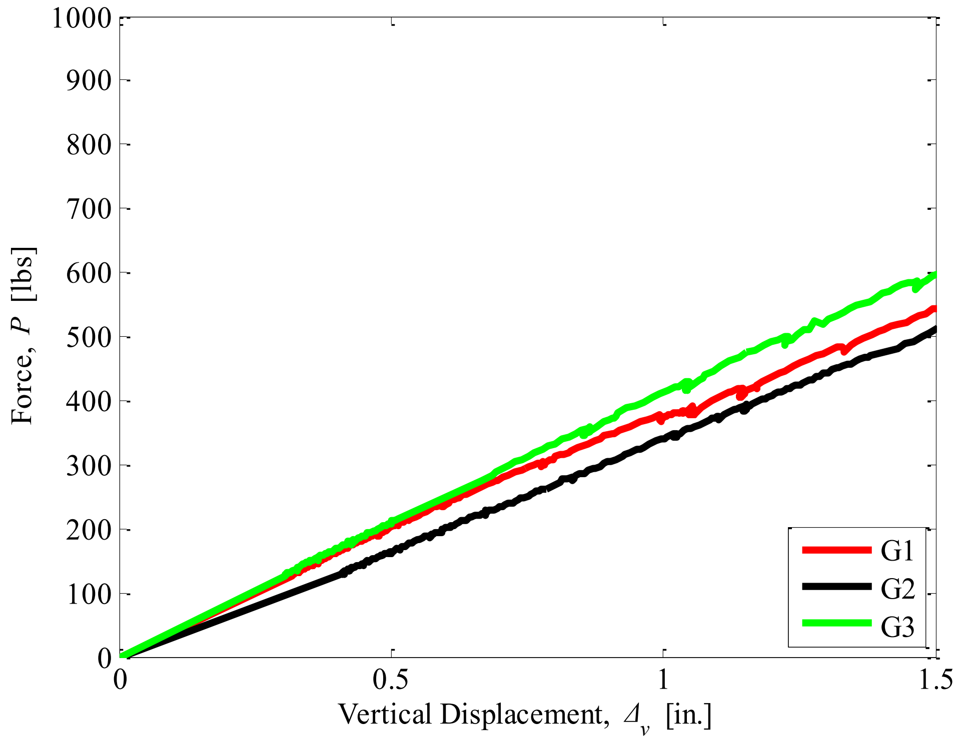
1000
900
800
700
600
500
400
300
200
100
0
0
0.5
1
1.5
Force, P [lbs]
Vertical Displacement, Δ_v [in.]
G1
G2
G3

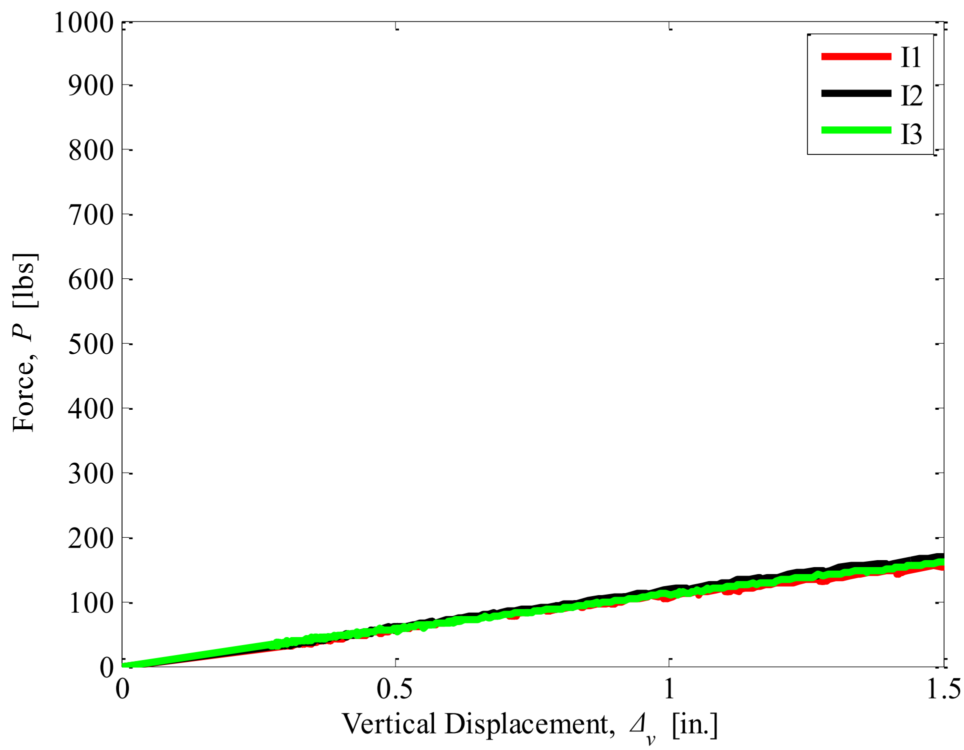
1000
900
800
700
600
500
400
300
200
100
0
0
0.5
1
1.5
Force, P [lbs]
Vertical Displacement, Δ_v [in.]
I1
I2
I3

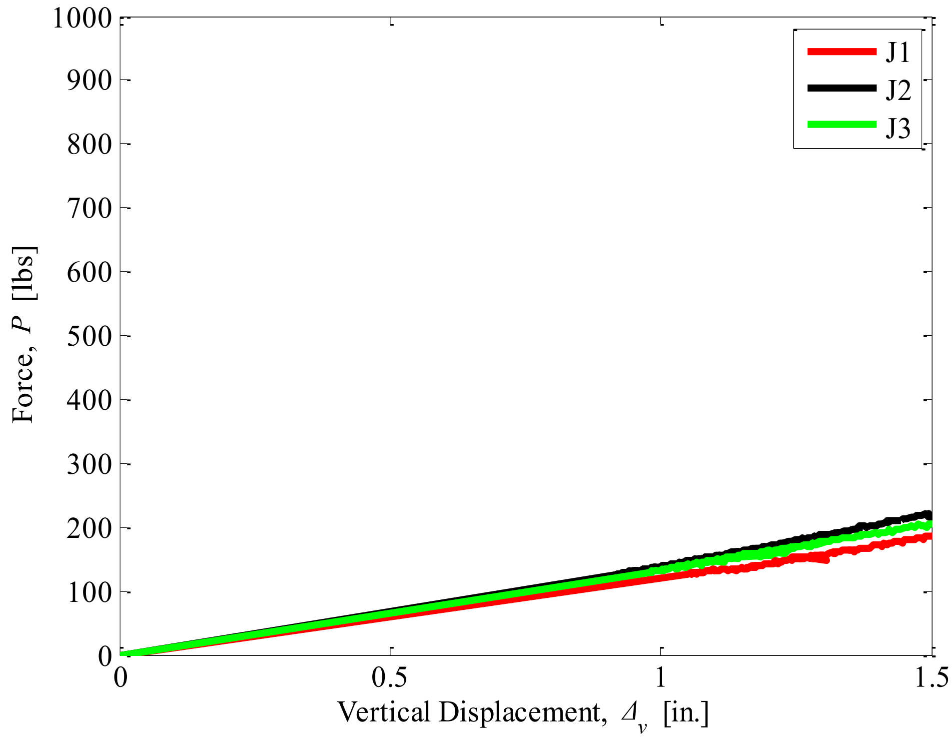
J1
J2
J3
Force, P [lbs]
Vertical Displacement, Δ_v [in.]
0
100
200
300
400
500
600
700
800
900
1000
0
0.5
1
1.5

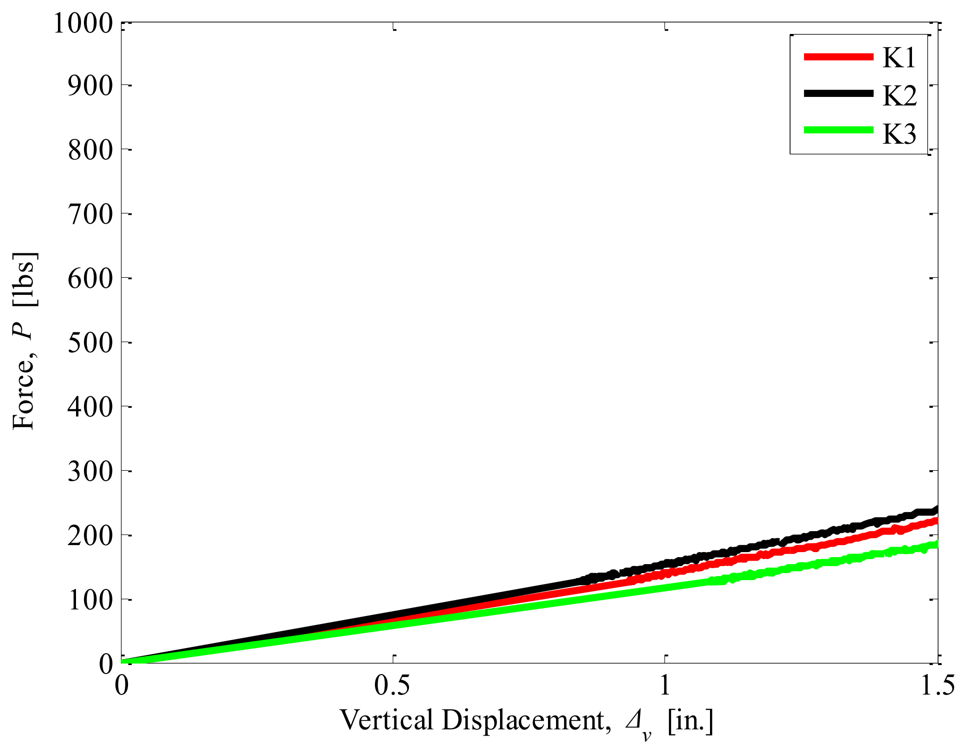
K1
K2
K3
Force, P [lbs]
Vertical Displacement, Δ_v [in.]
0
100
200
300
400
500
600
700
800
900
1000
0
0.5
1
1.5

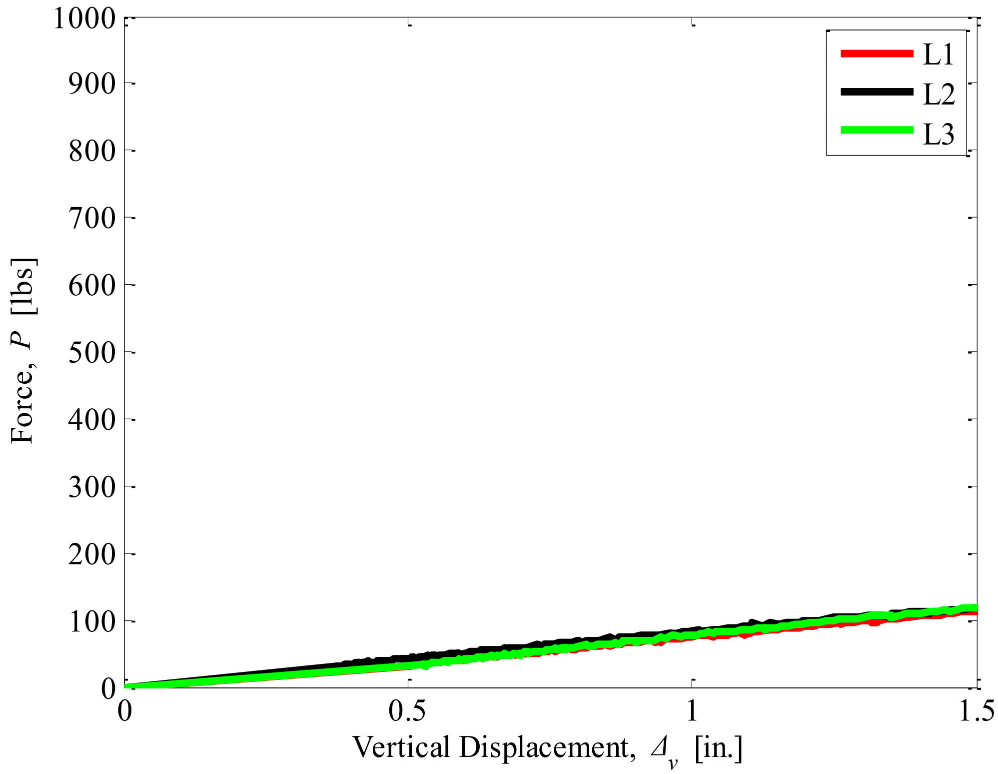
1000
900
800
700
600
500
400
300
200
100
0
Force, P [lbs]
0
0.5
1
1.5
Vertical Displacement, Δ_v [in.]
L1
L2
L3

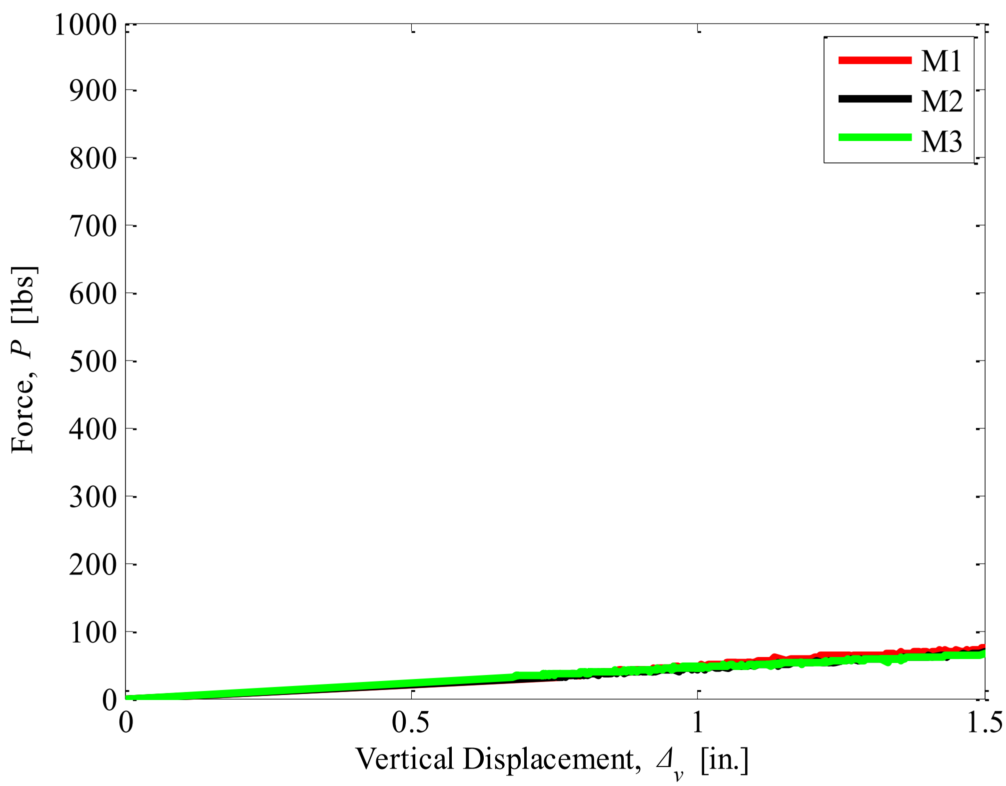
1000
900
800
700
600
500
400
300
200
100
0
Force, P [lbs]
0
0.5
1
1.5
Vertical Displacement, Δ_v [in.]
M1
M2
M3

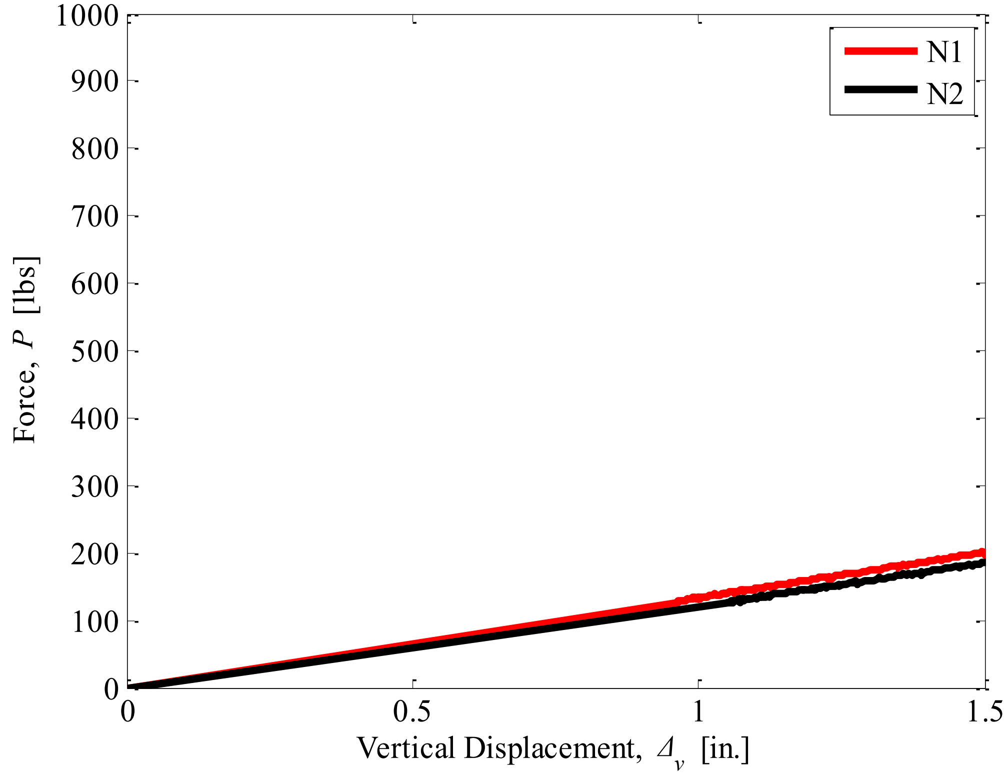

1000
900
800
700
600
500
400
300
200
100
0
Force, P [lbs]
0
0.5
1
1.5
Vertical Displacement, Δv [in.]
N1
N2

Testing Matrix

Panel Type	Test Number	Panel Thickness	Cold-formed Member	Member Type
CF-42 Mesa - concealed-fastener wall panel [42"]	A1	2"	C8-12 x 96"	Cee
	A2	2"	C8-12 x 96"	Cee
	A3	2"	C8-12 x 96"	Cee
	B1	4"	C8-12 x 96"	Cee
	B2	4"	C8-12 x 96"	Cee
	B3	4"	C8-12 x 96"	Cee
	C1	2"	Z8-12 x 96"	Zee
	C2	2"	Z8-12 x 96"	Zee
	C3	2"	Z8-12 x 96"	Zee
	D1	4"	Z8-12 x 96"	Zee
	D2	4"	Z8-12 x 96"	Zee
	D3	4"	Z8-12 x 96"	Zee
	E1	2"	Z8-16 x 96"	Zee
	E2	2"	Z8-16 x 96"	Zee
	E3	2"	Z8-16 x 96"	Zee
CFR-42 - Standing seam concealed-fastener roof panel [42"]	F1	2"	Z8-12 x 96"	Zee
	F2	2"	Z8-12 x 96"	Zee
	F3	2"	Z8-12 x 96"	Zee
	G1	4"	Z8-12 x 96"	Zee
	G2	4"	Z8-12 x 96"	Zee
	G3	4"	Z8-12 x 96"	Zee
LS-36 - Through-fastened panel - wall attachment [36"]	H1	2"	Z8-12 x 36"	Zee
	H2	2"	Z8-12 x 36"	Zee
	H3	2"	Z8-12 x 36"	Zee
	I1	4"	Z8-12 x 36"	Zee
	I2	4"	Z8-12 x 36"	Zee
	I3	4"	Z8-12 x 36"	Zee
DM40 - Concealed-fastener wall panel [40"]	J1	2"	Z8-16 x 92"	Zee
	J2	2"	Z8-16 x 92"	Zee
	J3	2"	Z8-16 x 92"	Zee
	K1	4"	Z8-16 x 92"	Zee
	K2	4"	Z8-16 x 92"	Zee
	K3	4"	Z8-16 x 92"	Zee
HR3 - Through-fastened roof panel [40"]	L1	4"	Z8-12 x 36"	Zee
	L2	4"	Z8-12 x 36"	Zee
	L3	4"	Z8-12 x 36"	Zee
	M1	4"	Z12-12 x 36"	Zee
	M2	4"	Z12-12 x 36"	Zee
	M3	4"	Z12-12 x 36"	Zee
SR2 - Standing seam concealed-fastener roof panel [40"]	N1	4"	Z12-12 x 92"	Zee
	N2	4"	Z12-12 x 92"	Zee
	N3	4"	Z12-12 x 92"	Zee

Appendix B - Load vs. Horizontal panel deflection, Δ_h

The following charts show the results for panel horizontal deflection measured behavior for the point moment loading provided by total load P (applied tension load plus spreader bar weight) applied eccentrically. Results of like tests using identical cold-formed member depths and thicknesses, panel types, and overall panel thicknesses are shown on the same chart. A reprint of the matrix showing the parameters used each test can be found at the end of Appendix A.

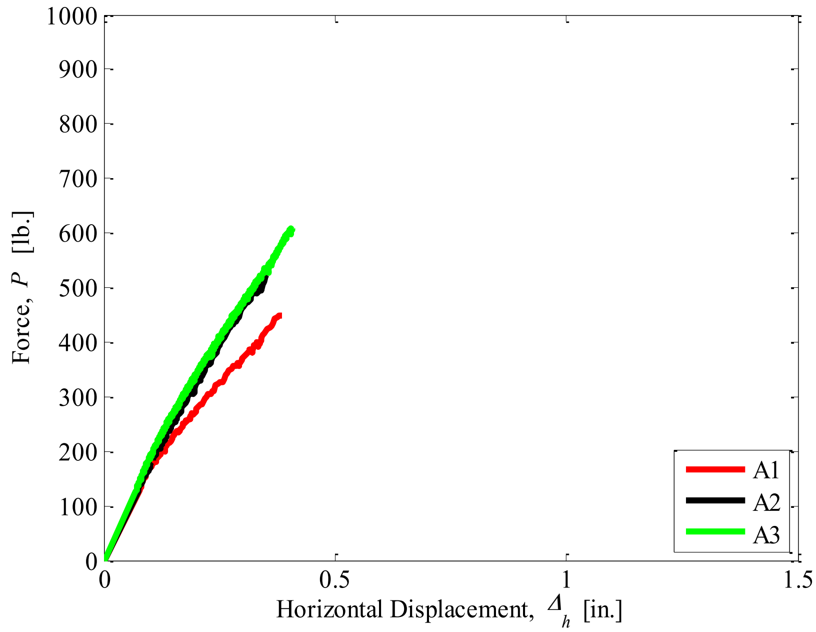

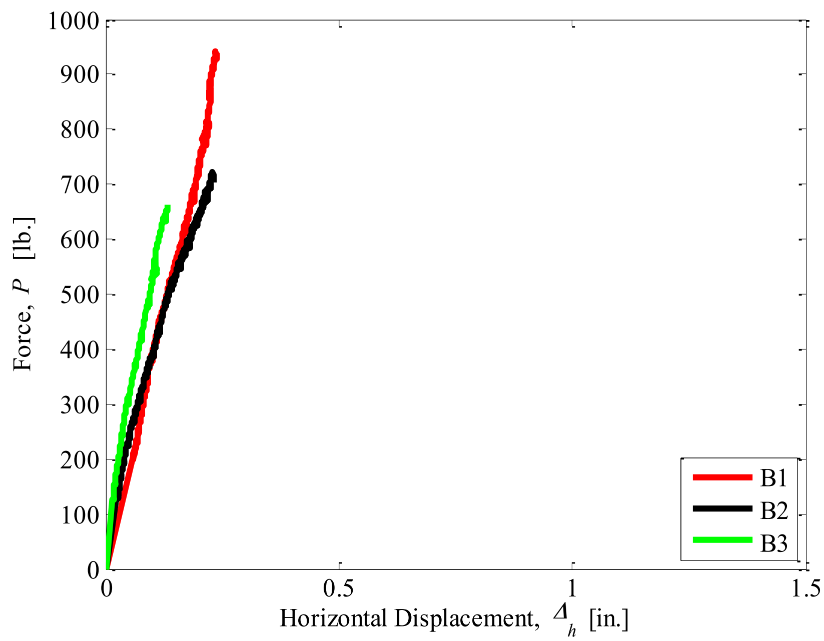

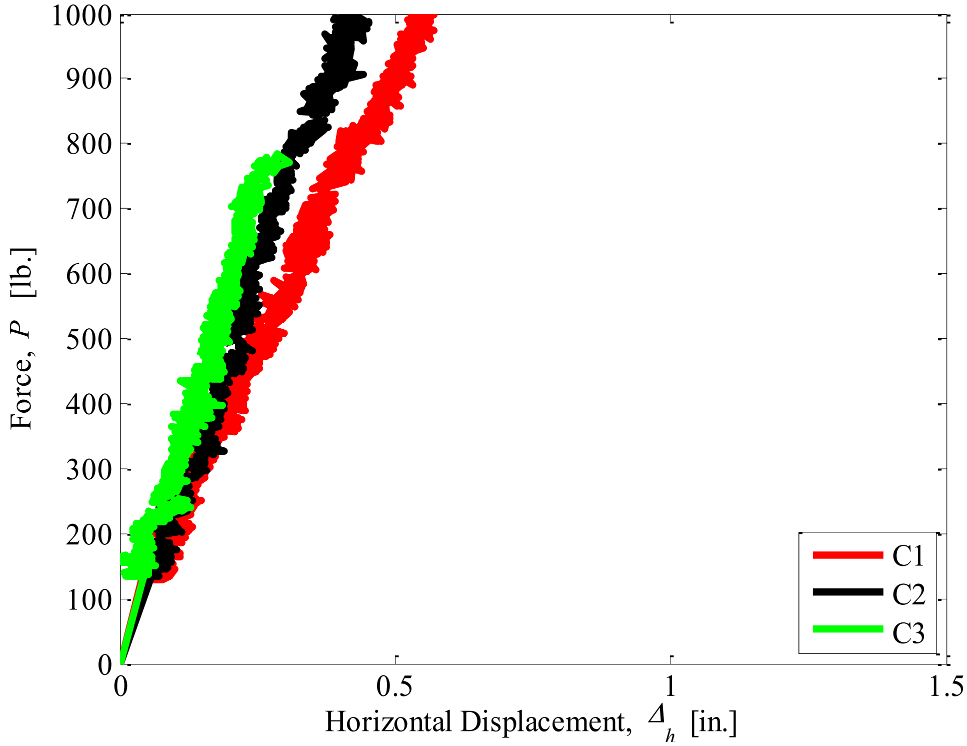
1000
900
800
700
600
500
400
300
200
100
0
Force, P [lb.]
0
0.5
1
1.5
Horizontal Displacement, Δ_h [in.]
C1
C2
C3

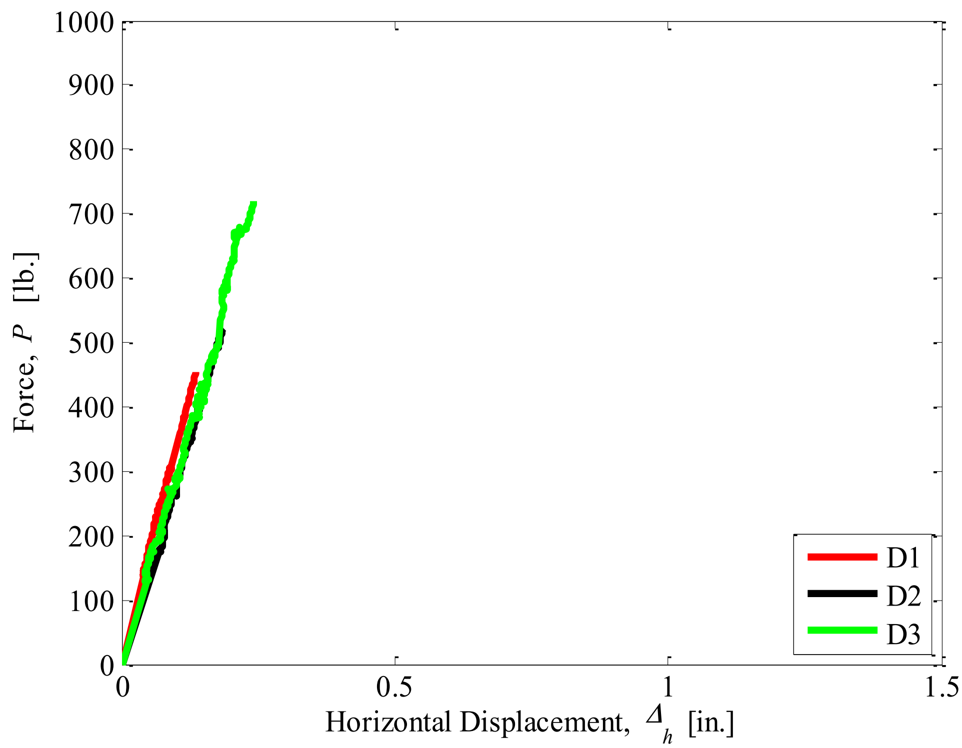
1000
900
800
700
600
500
400
300
200
100
0
Force, P [lb.]
0
0.5
1
1.5
Horizontal Displacement, Δ_h [in.]
D1
D2
D3

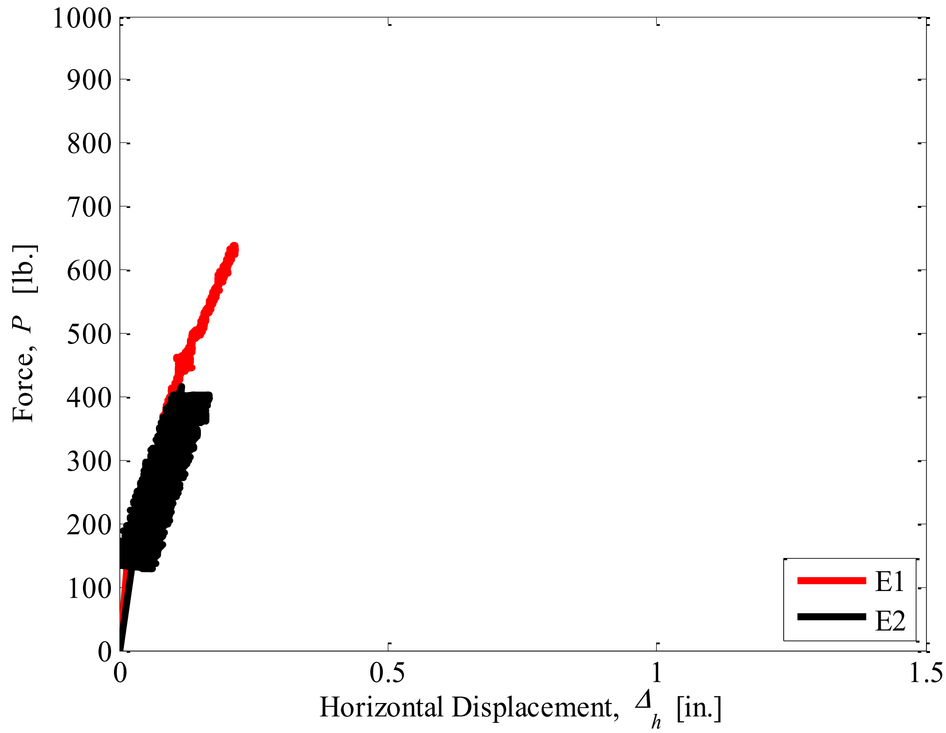

Force, P [lb.]
Horizontal Displacement, Δh [in.]
E1
E2

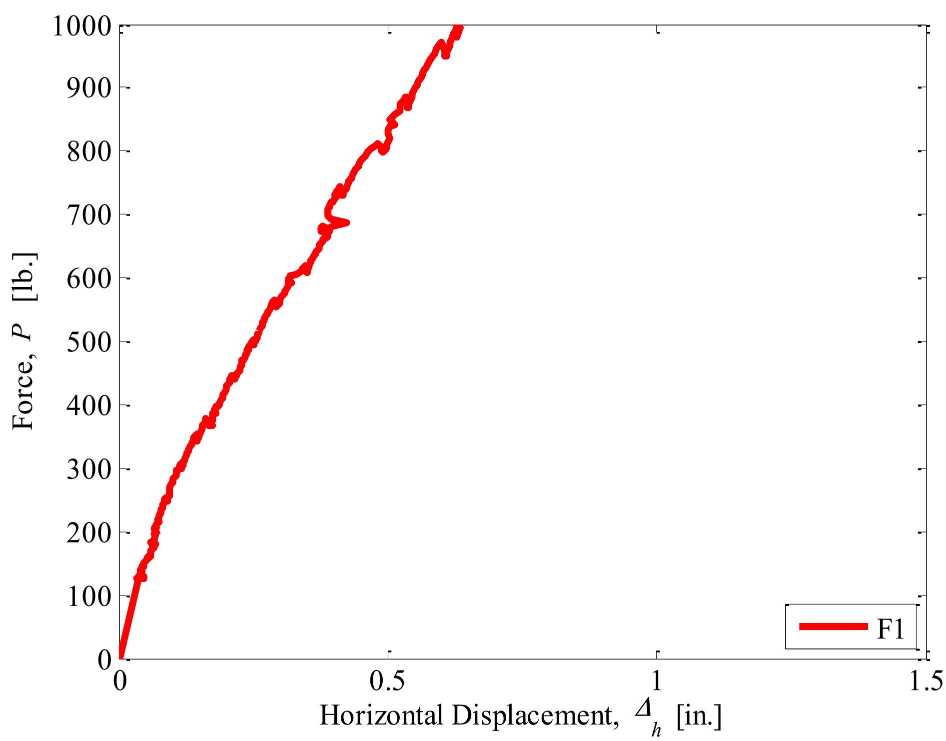

Force, P [lb.]
Horizontal Displacement, Δh [in.]
F1

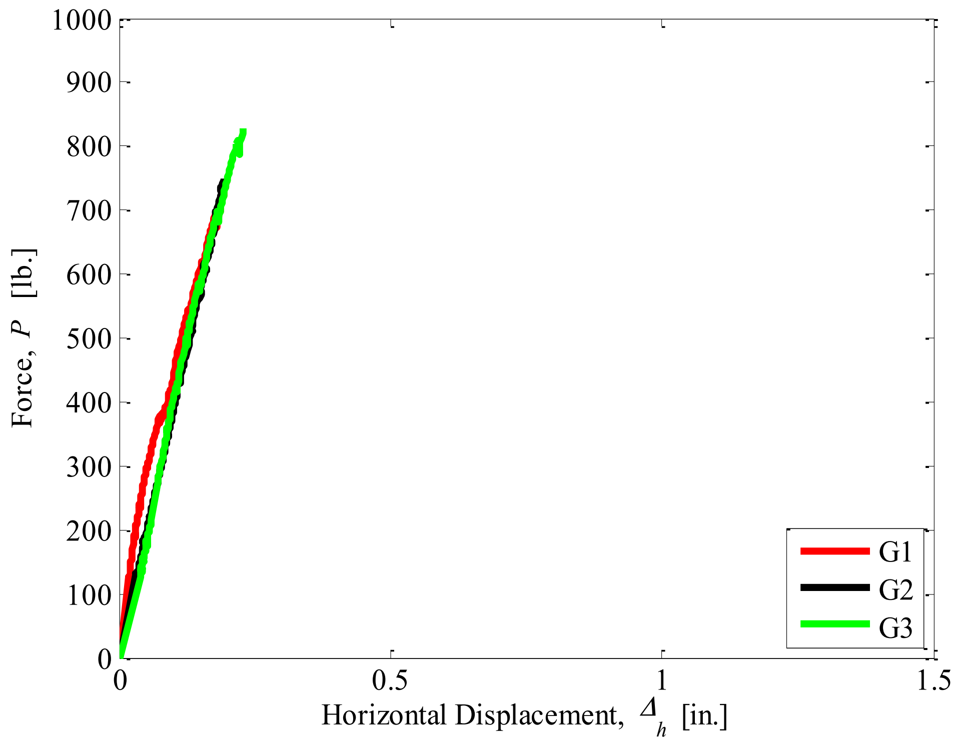
1000
900
800
700
600
500
400
300
200
100
0
Force, P [lb.]
0
0.5
1
1.5
Horizontal Displacement, Δ_h [in.]
G1
G2
G3

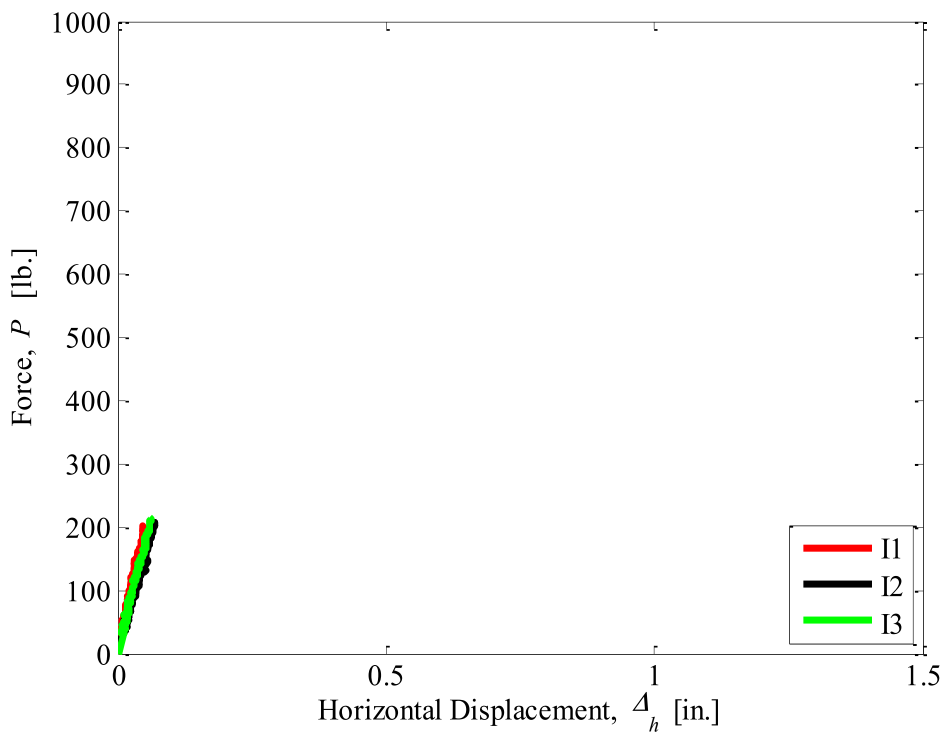
1000
900
800
700
600
500
400
300
200
100
0
Force, P [lb.]
0
0.5
1
1.5
Horizontal Displacement, Δ_h [in.]
I1
I2
I3

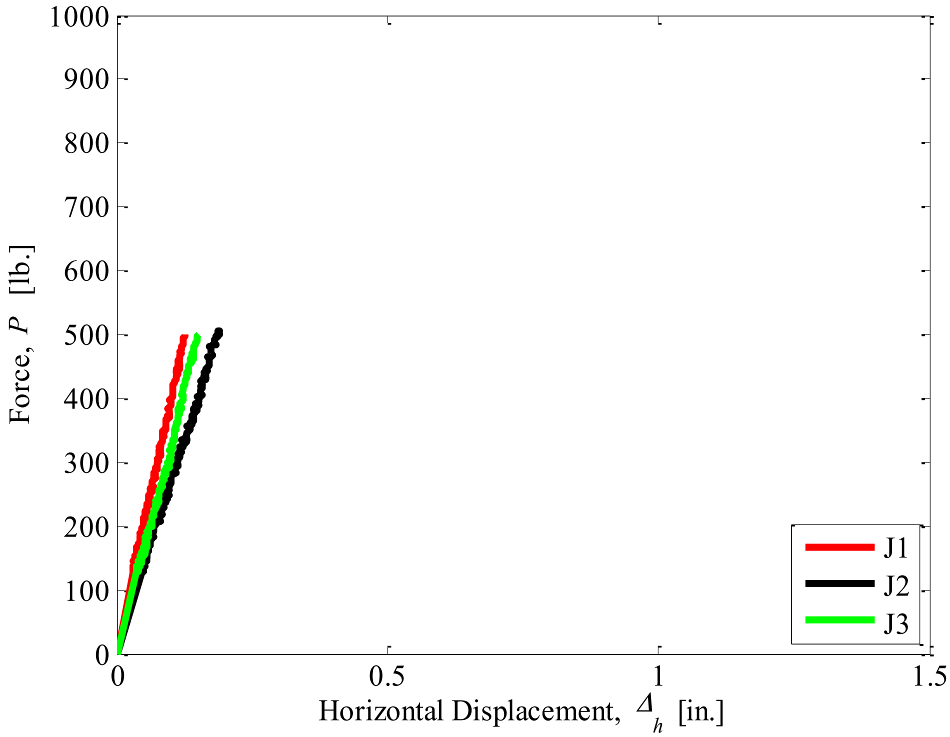
Force, P [lb.]
Horizontal Displacement, Δ_h [in.]
J1
J2
J3

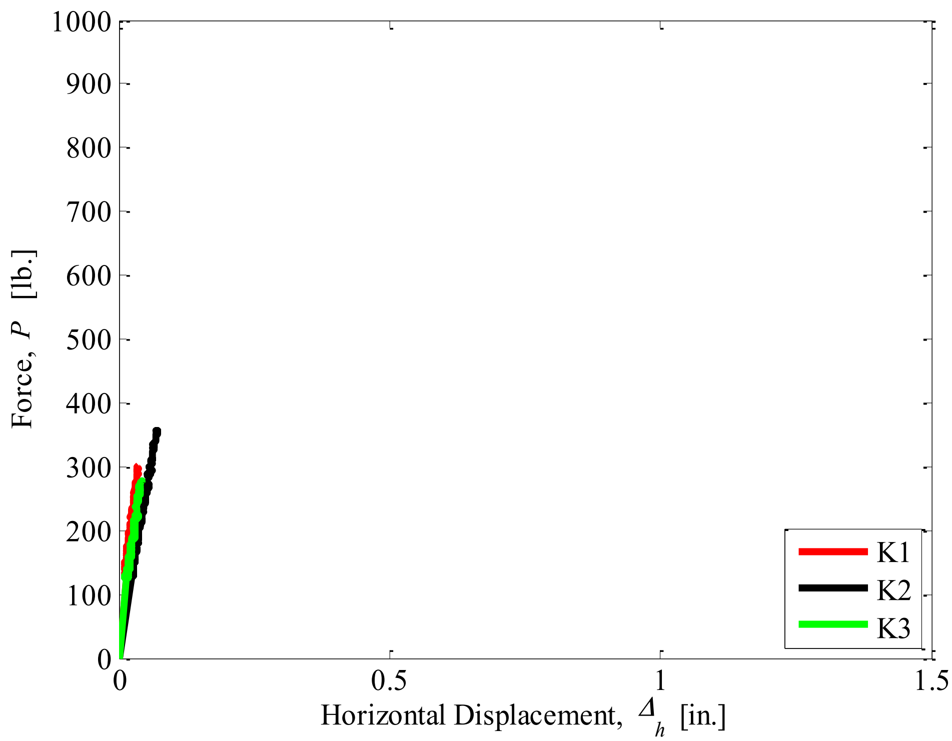
Force, P [lb.]
Horizontal Displacement, Δ_h [in.]
K1
K2
K3

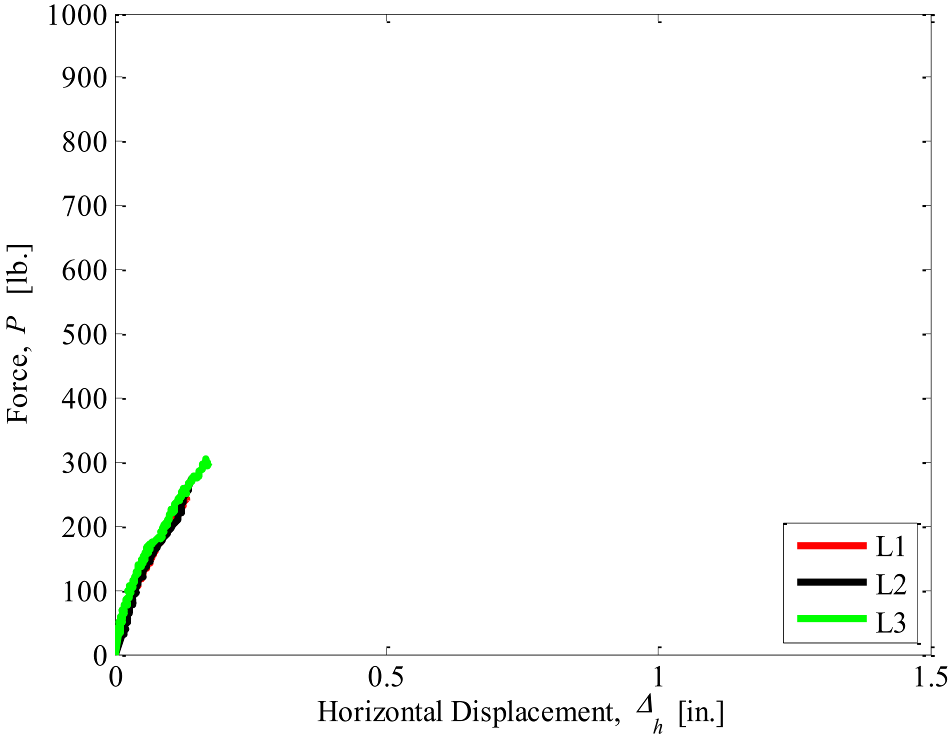

1000
900
800
700
600
500
400
300
200
100
0
Force, P [lb.]
0
0.5
1
1.5
Horizontal Displacement, Δ_h [in.]
L1
L2
L3

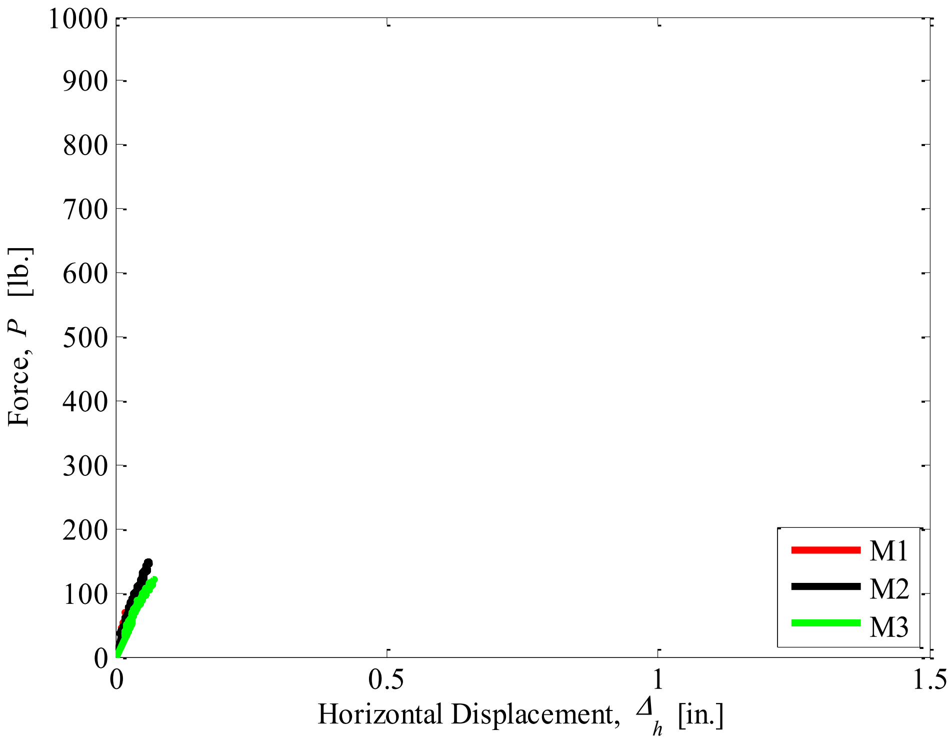

1000
900
800
700
600
500
400
300
200
100
0
Force, P [lb.]
0
0.5
1
1.5
Horizontal Displacement, Δ_h [in.]
M1
M2
M3

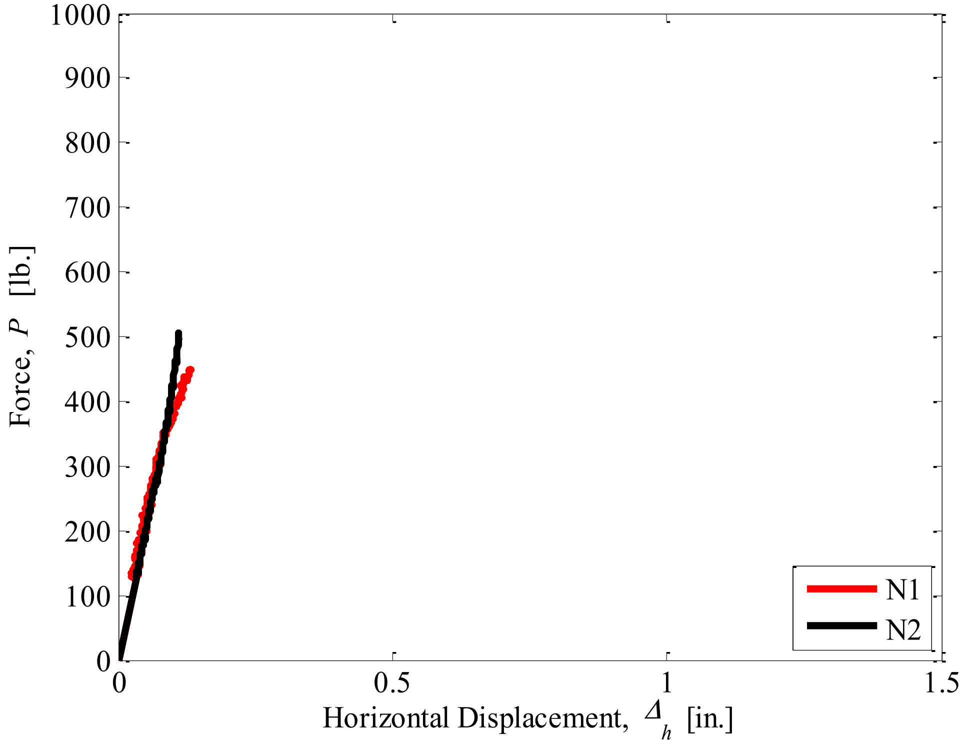
1000
900
800
700
600
500
400
300
200
100
0
0
0.5
1
1.5
Force, P [lb.]
Horizontal Displacement, Δh [in.]
N1
N2

Appendix C - Load vs. vertical fastened flange deflection, Δ_t

The following charts show the measured results for vertical deflection of the attached cold-formed member flange with total load P (applied tension load plus spreader bar weight). Results of like tests using identical cold-formed member depths and thicknesses, panel types, and overall panel thicknesses are shown on the same chart. A reprint of the matrix showing the parameters used each test can be found at the end of Appendix A.

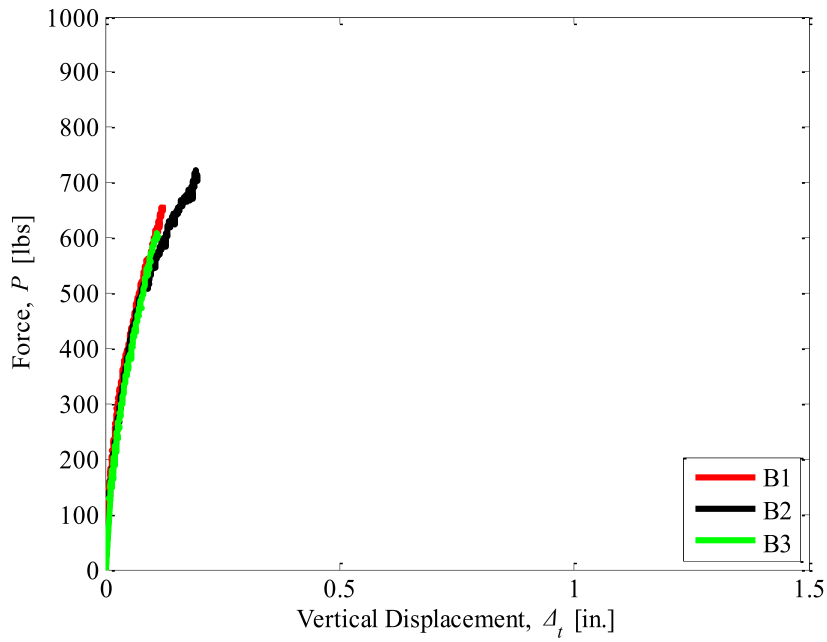

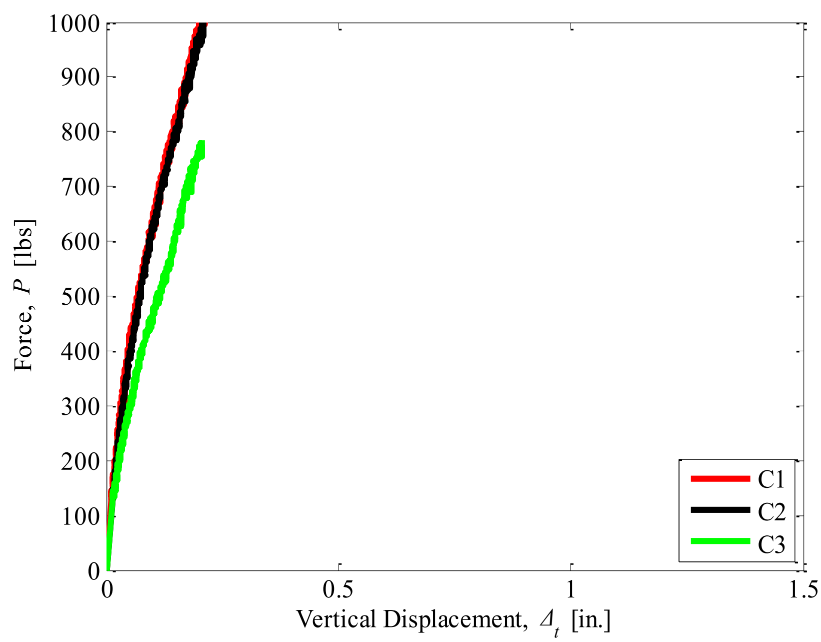

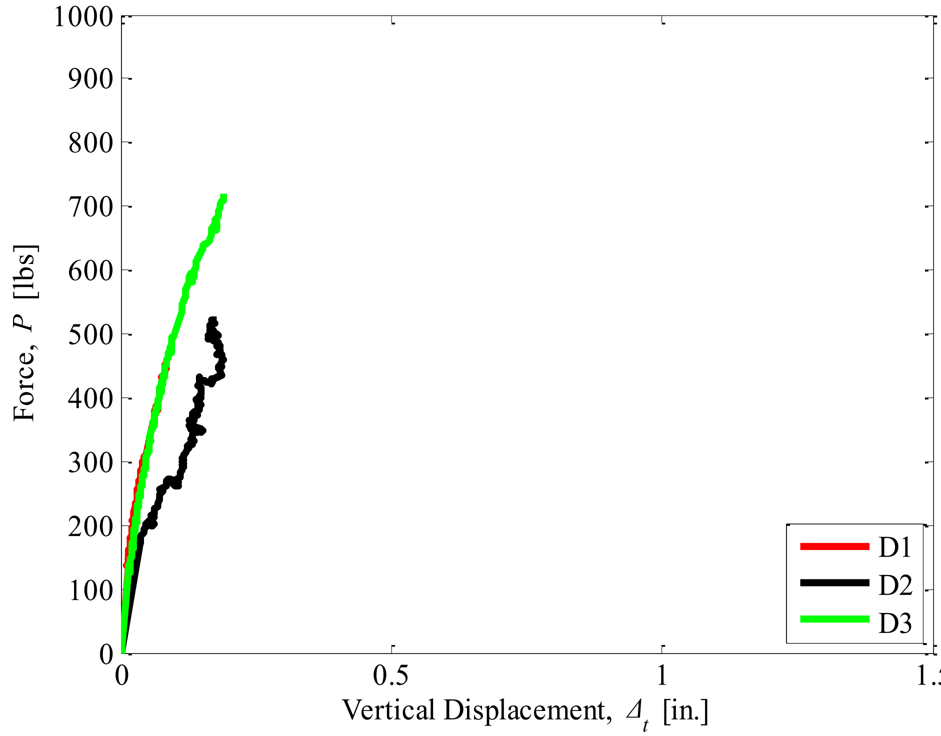
1000
900
800
700
600
500
400
300
200
100
0
0
0.5
1
1.5
Force, P [lbs]
Vertical Displacement, Δ_t [in.]
D1
D2
D3

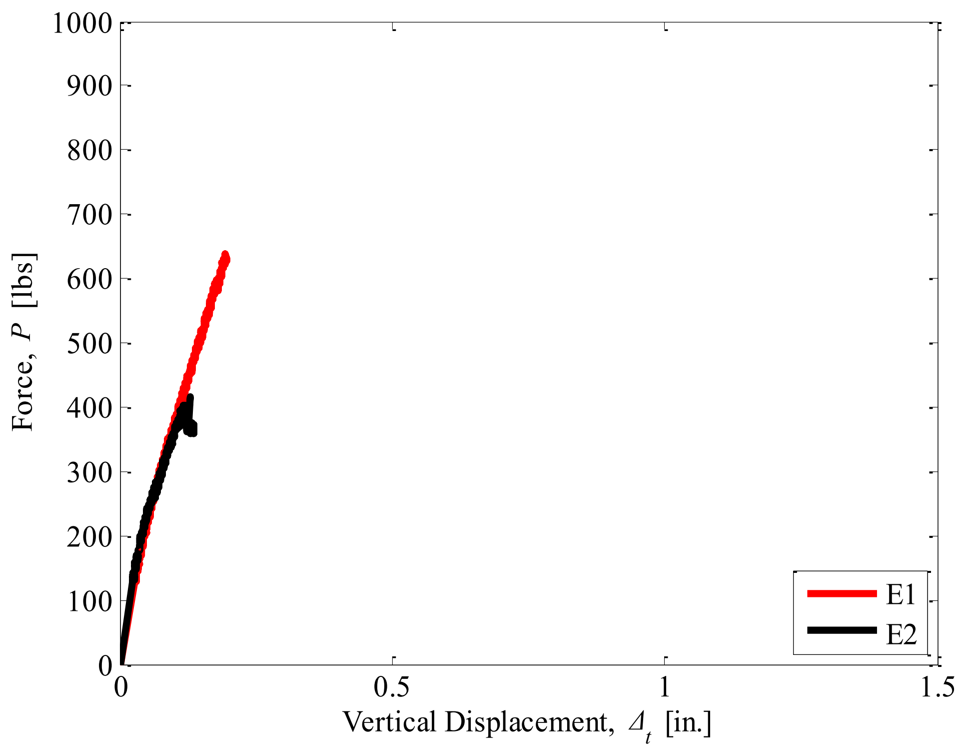
1000
900
800
700
600
500
400
300
200
100
0
0
0.5
1
1.5
Force, P [lbs]
Vertical Displacement, Δ_t [in.]
E1
E2

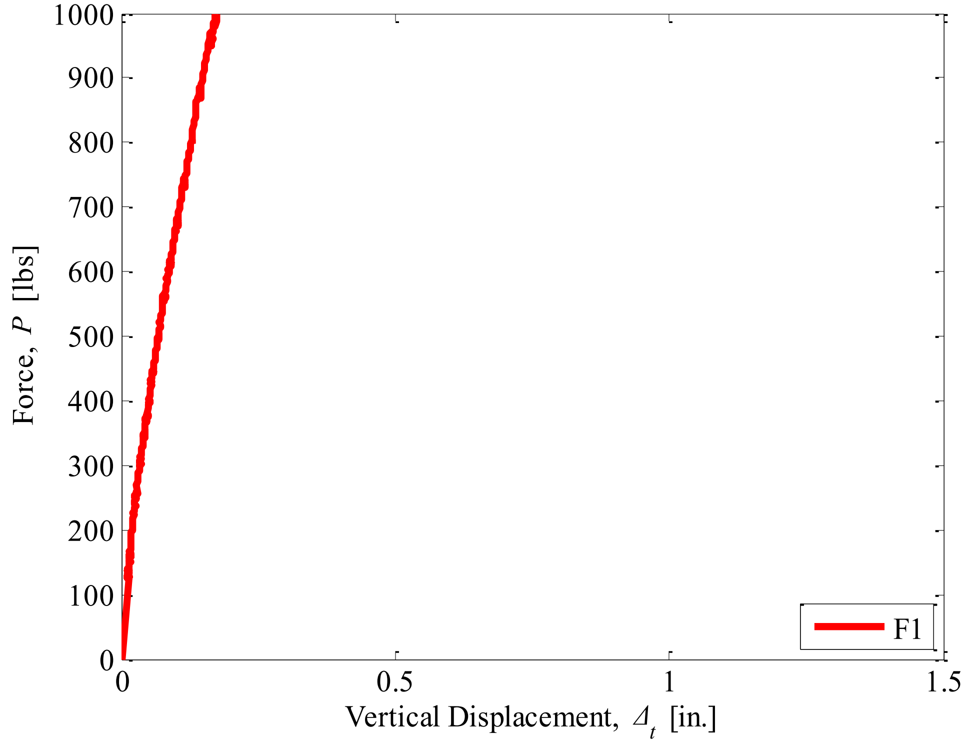

1000
900
800
700
600
500
400
300
200
100
0
Force, P [lbs]
F1
0
0.5
1
1.5
Vertical Displacement, Δ_t [in.]

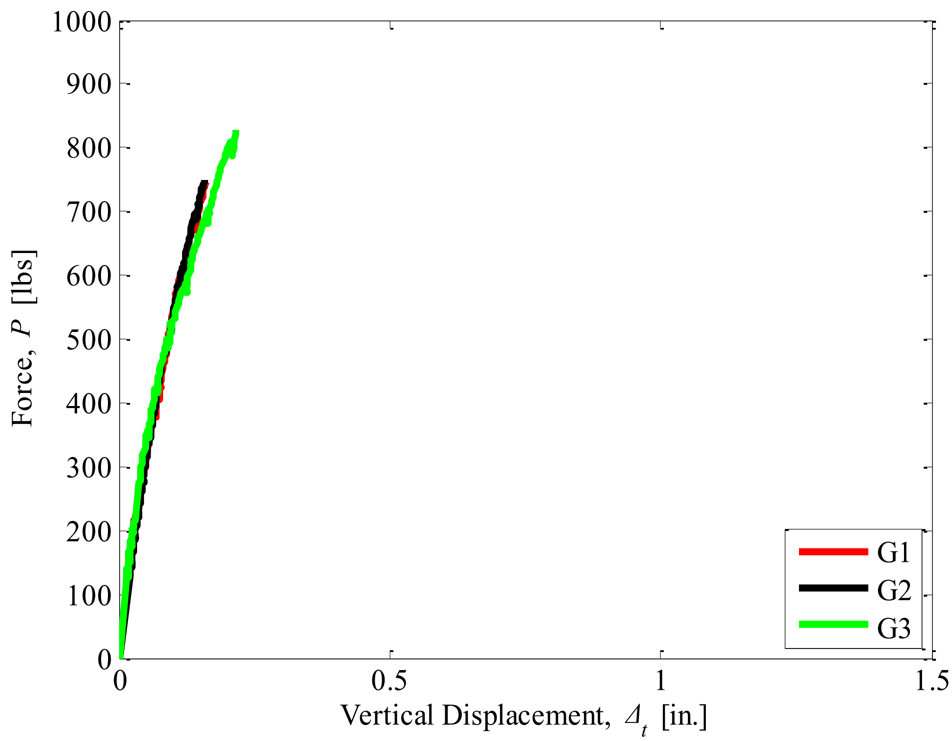

1000
900
800
700
600
500
400
300
200
100
0
Force, P [lbs]
G1
G2
G3
0
0.5
1
1.5
Vertical Displacement, Δ_t [in.]

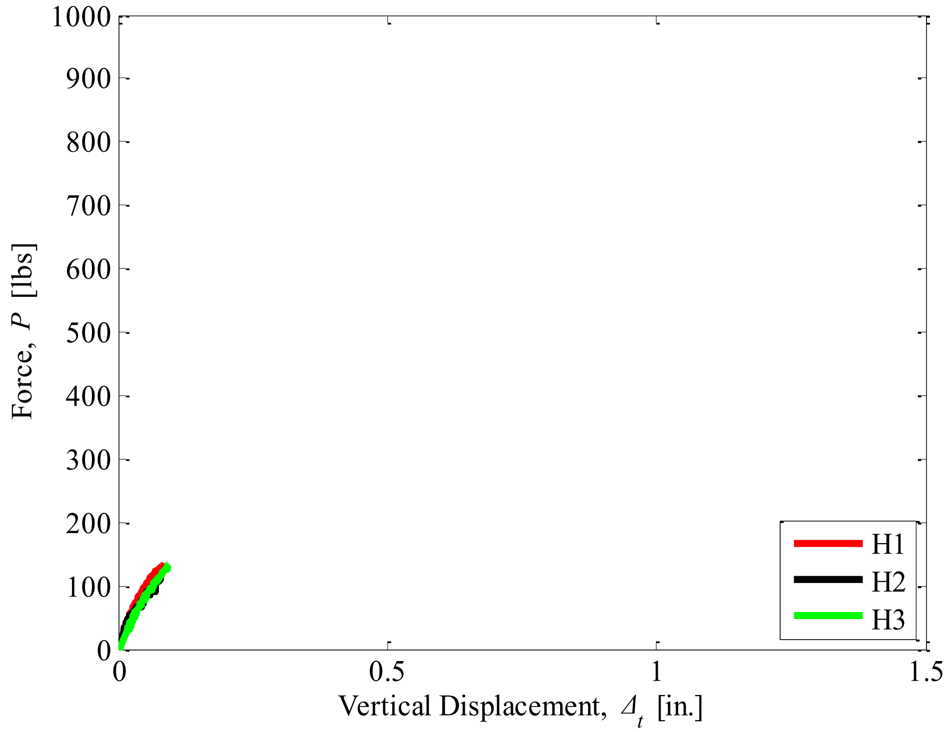
Force, P [lbs]
Vertical Displacement, Δ_t [in.]
H1
H2
H3

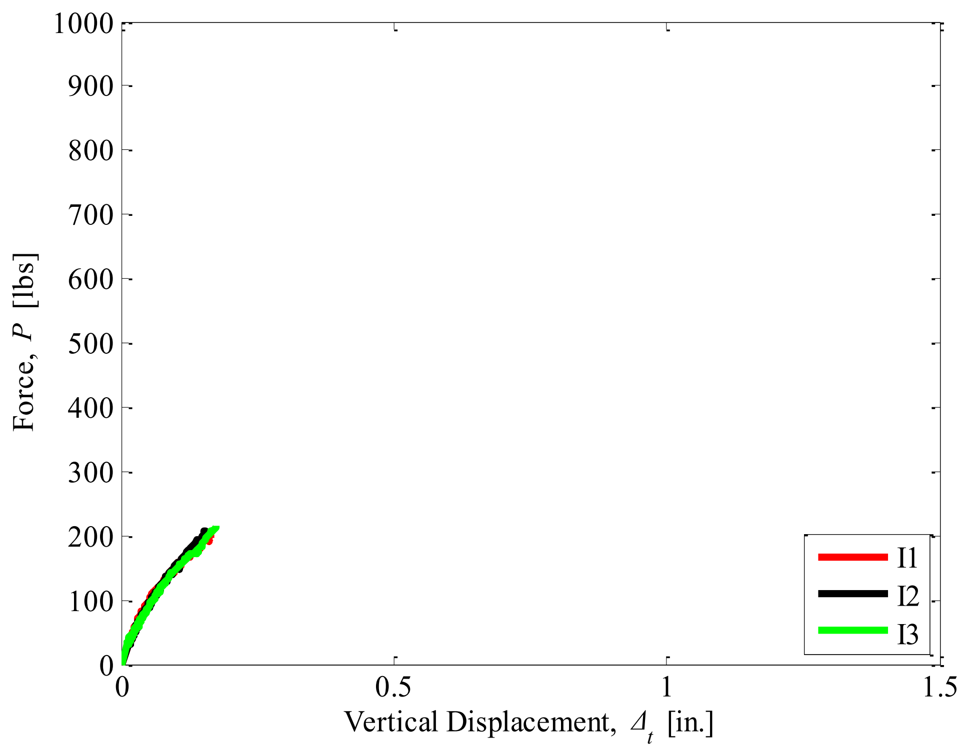
Force, P [lbs]
Vertical Displacement, Δ_t [in.]
I1
I2
I3

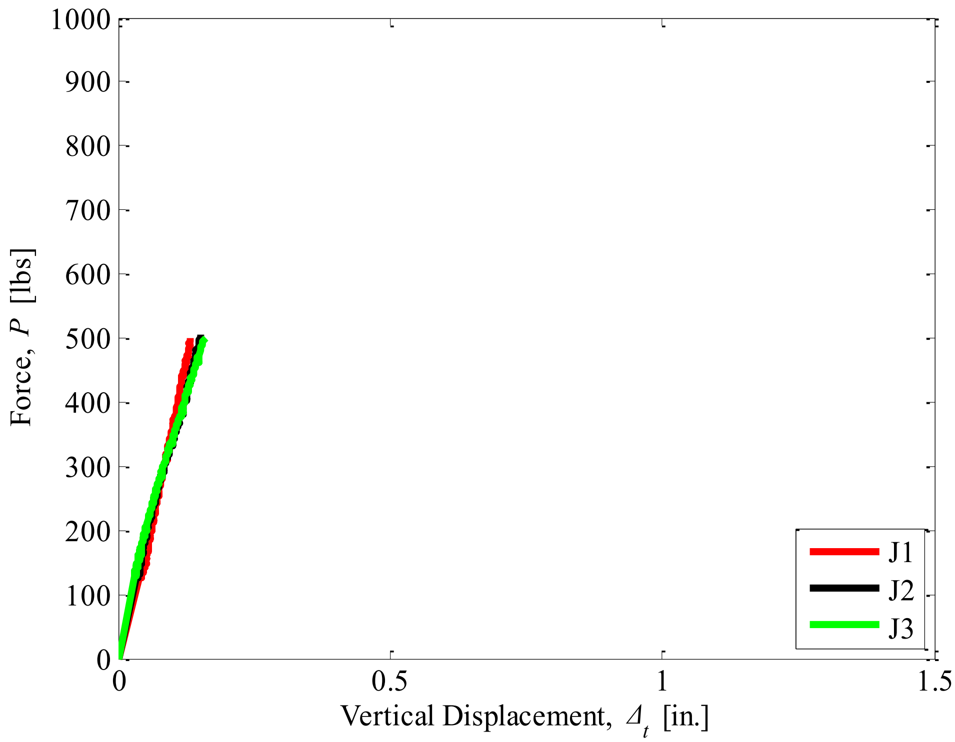
1000
900
800
700
600
500
400
300
200
100
0
Force, P [lbs]
0
0.5
1
1.5
Vertical Displacement, Δ_t [in.]
J1
J2
J3

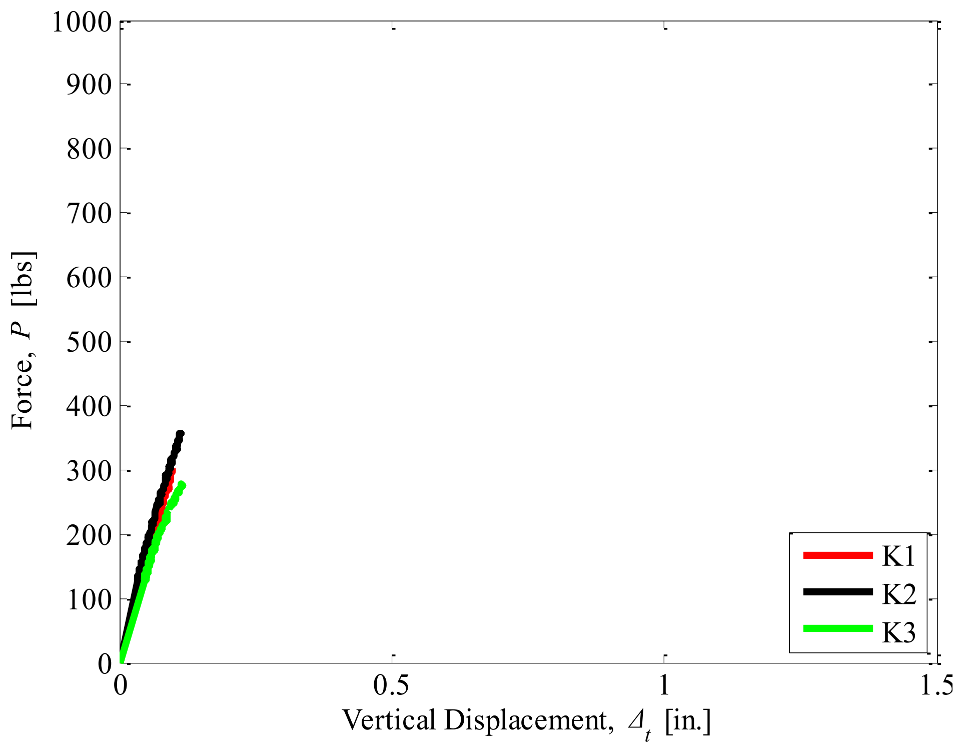
1000
900
800
700
600
500
400
300
200
100
0
Force, P [lbs]
0
0.5
1
1.5
Vertical Displacement, Δ_t [in.]
K1
K2
K3

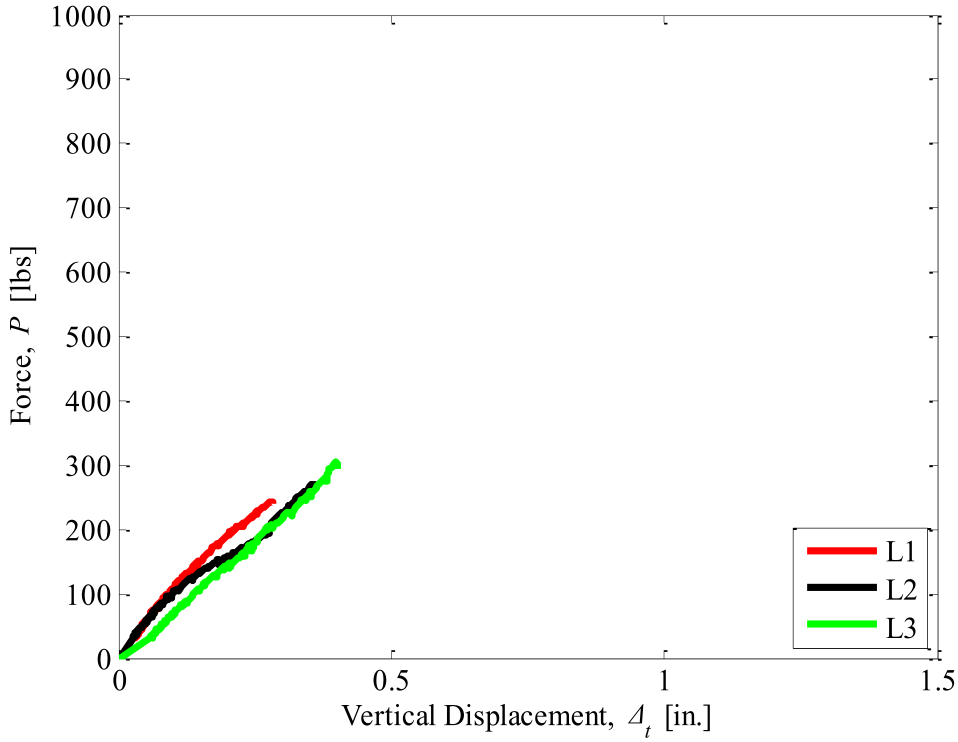
Force, P [lbs]
Vertical Displacement, Δ_t [in.]
L1
L2
L3

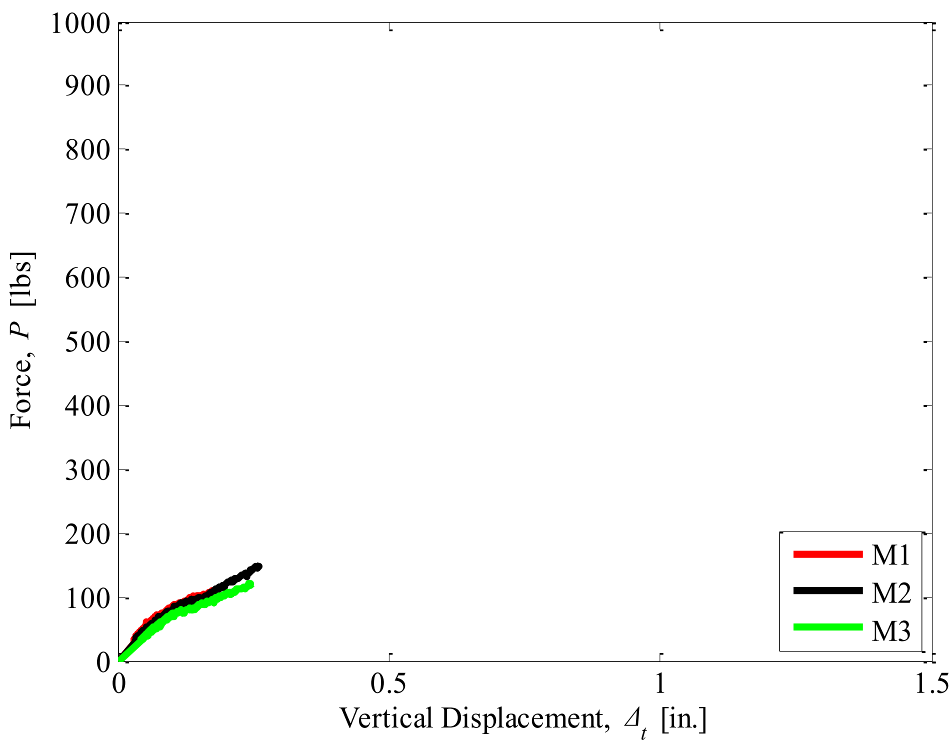
Force, P [lbs]
Vertical Displacement, Δ_t [in.]
M1
M2
M3

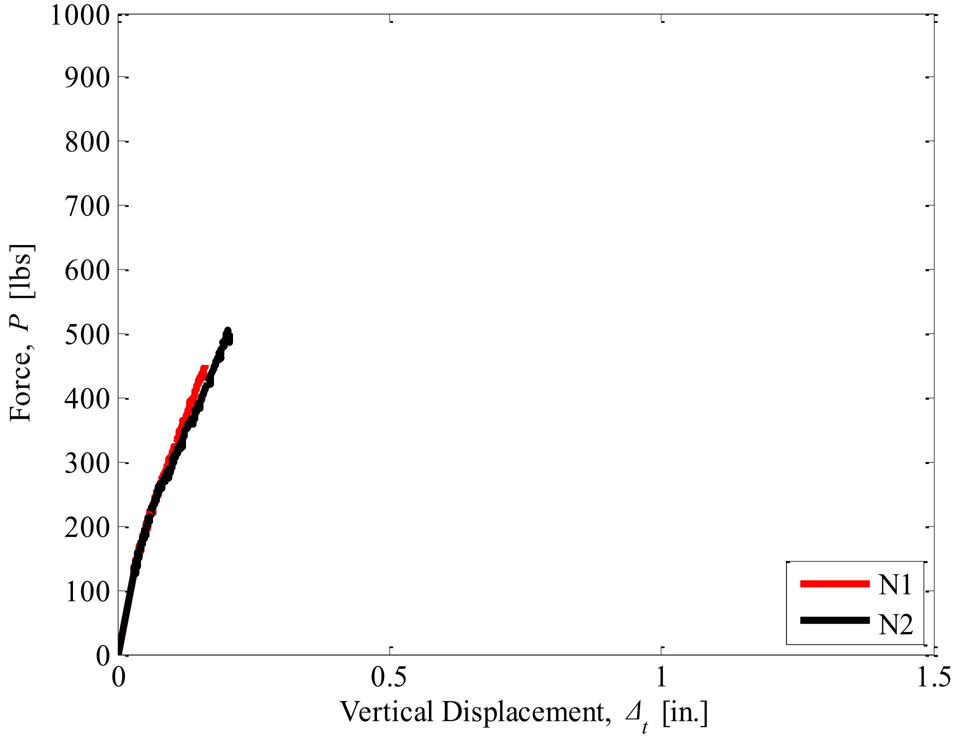

1000
900
800
700
600
500
400
300
200
100
0
0
0.5
1
1.5
Force, P [lbs]
Vertical Displacement, Δ_t [in.]
N1
N2

Appendix D - Moment vs. connection rotation θ_ϕ for all test groups

The following chart shows the variation in average connection rotation with applied connection moment for all test groups. A detailed discussion of the reasons behind the different responses for the groups is included in the body of the report.

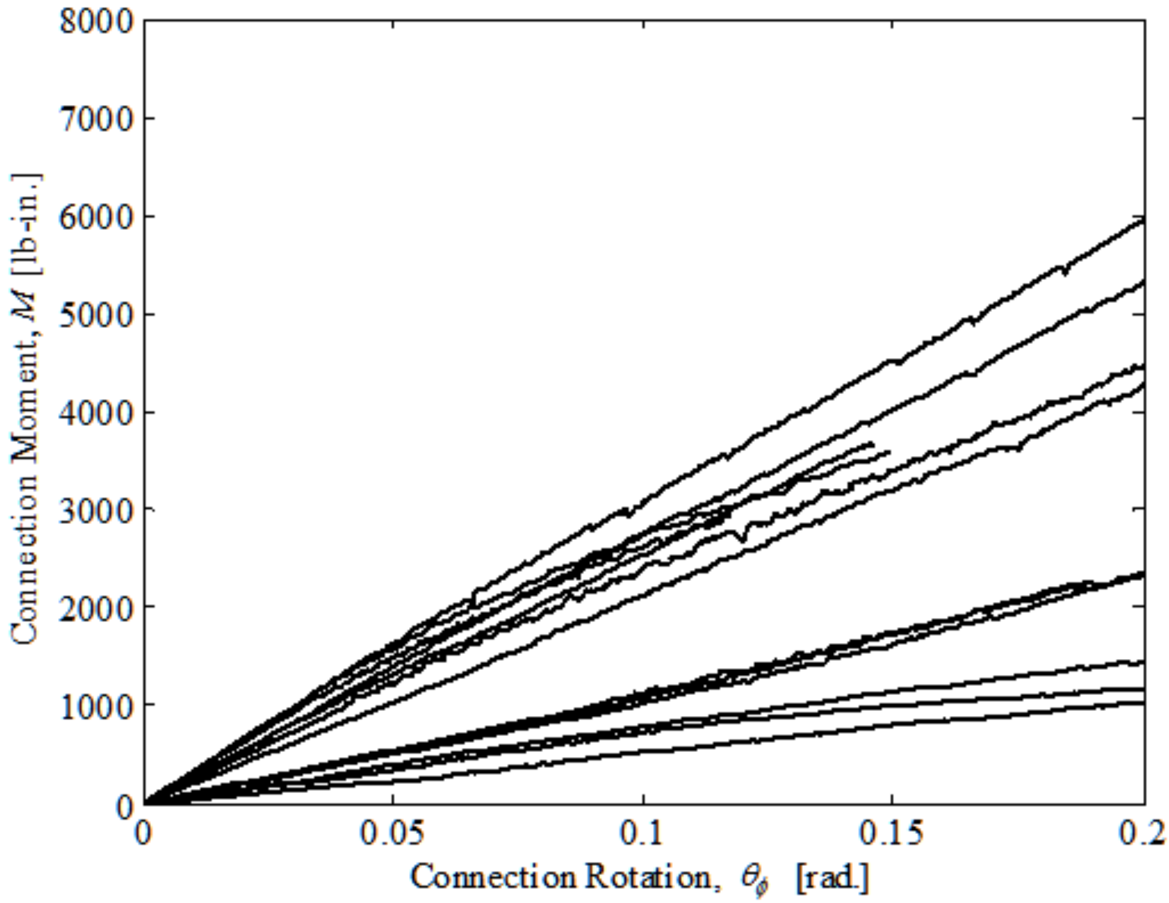

Appendix E - Moment vs. panel rotation, θ_p for all test groups

The following chart shows the average panel rotation angle at the c old-formed member connection for all test groups. Note that the panel rotation component comprised only a small portion of the total cold-formed structural member deflection in the testing.

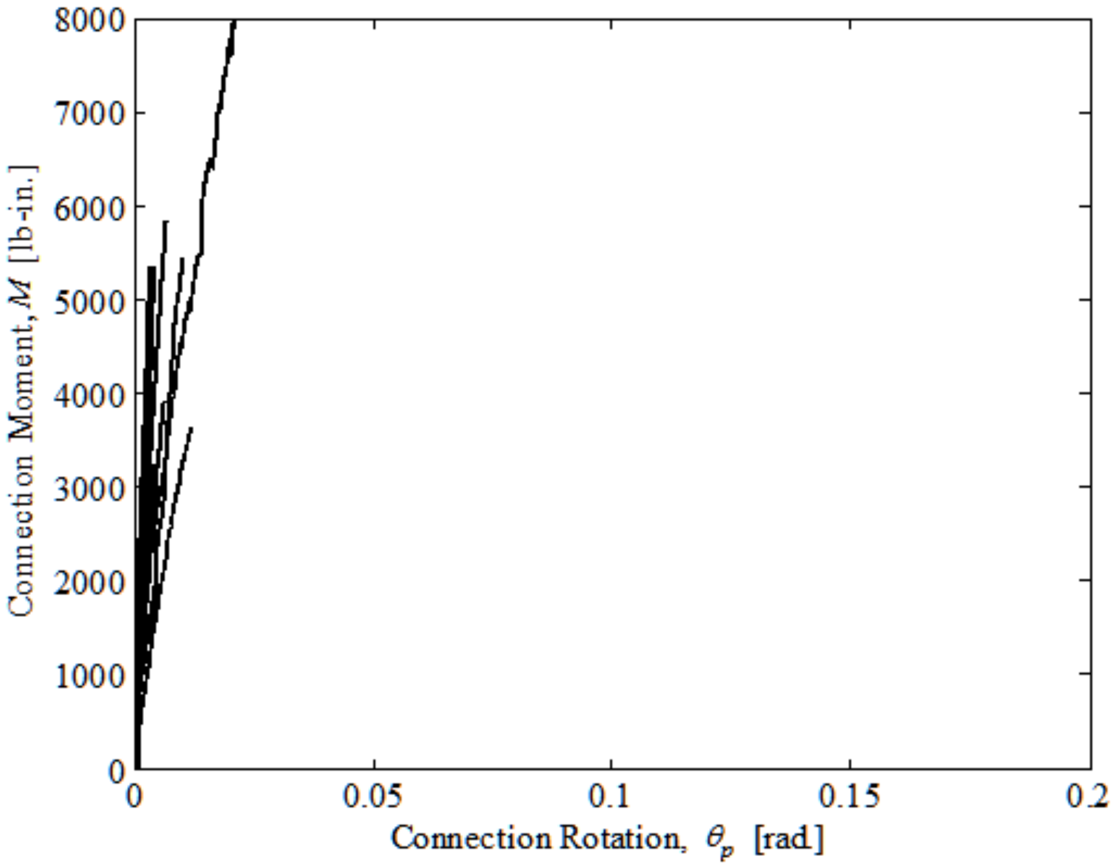

Appendix F – Rotational and translational stiffness calculations

Rotational stiffness

By following equations 1 to 4 in the main body of the report, rotation stiffness can be determined as shown. For this example, the P vs. Δ_v and Δ_h data from test A1 have been reproduced in Figure 20 below.

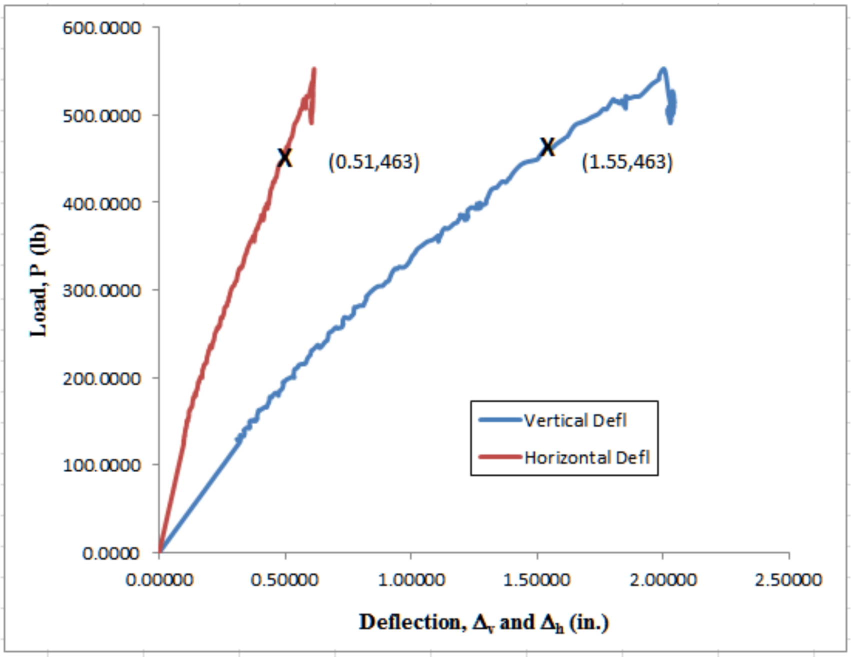

Figure 20: (a) Force vs. Δ_v and Δ_h displacement data for test A1

$$\theta = \frac{\Delta_v}{h_0} = \frac{1.55in.}{8.00in.} = 0.194\ rad. \qquad \text{(from Eqn 2)}$$

$$\theta_p = \frac{2\Delta_h L_1}{L_2^{\,2}} = \frac{2(0.51in.)(57.25in.)}{(54in.)^2} = 0.020\ rad. \qquad \text{(from Eqn 3)}$$

$$\theta_w = \frac{(P/L)h_o^2}{3EI_w} = \frac{(463/96)(8)^2}{3(2.95E7)(0.1023^3/12)} rad. = 0.0391\ rad. \qquad \text{(from Eqn 4)}$$

$$\theta_\phi = \Delta_v / h_o - \theta_p - \theta_w = 0.135\ rad.$$

$$k_\phi = \frac{(P/L)h_o}{\theta_\phi} = \frac{(463lbs/96in.)(8in.)}{0.135rad.} = 286.6\ \ lbs - in./rad./in. \qquad \text{(from Eqn 1)}$$

Translational stiffness

Using the method discussed in Section 2.2, translational stiffness can be calculated as shown below. The P vs. Δ_t chart from test C1 is reproduced in Figure 21 below.

$$Q_1 = \frac{P_1}{L} = \frac{127.5lbs}{96in.} = 1.328\ lbs/in.$$

$$Q_2 = \frac{P_2}{L} = \frac{372.1lbs}{96in.} = 3.876\ lbs/in.$$

$$k_x = \frac{Q_2 - Q_1}{\Delta_{t2} - \Delta_{t1}} = \frac{(3.876 - 1.328)lbs/in.}{(0.0438 - 0.0115)in.} = 78.9\ lbs/in./in.$$

Note that the initial portion of the curve is not used to avoid undue influence of the spreader weight preset load on the IMP translational stiffness behavior. The stiffness relationship can be approximated between the two points shown as linear with little loss of efficiency or lack of conservatism.

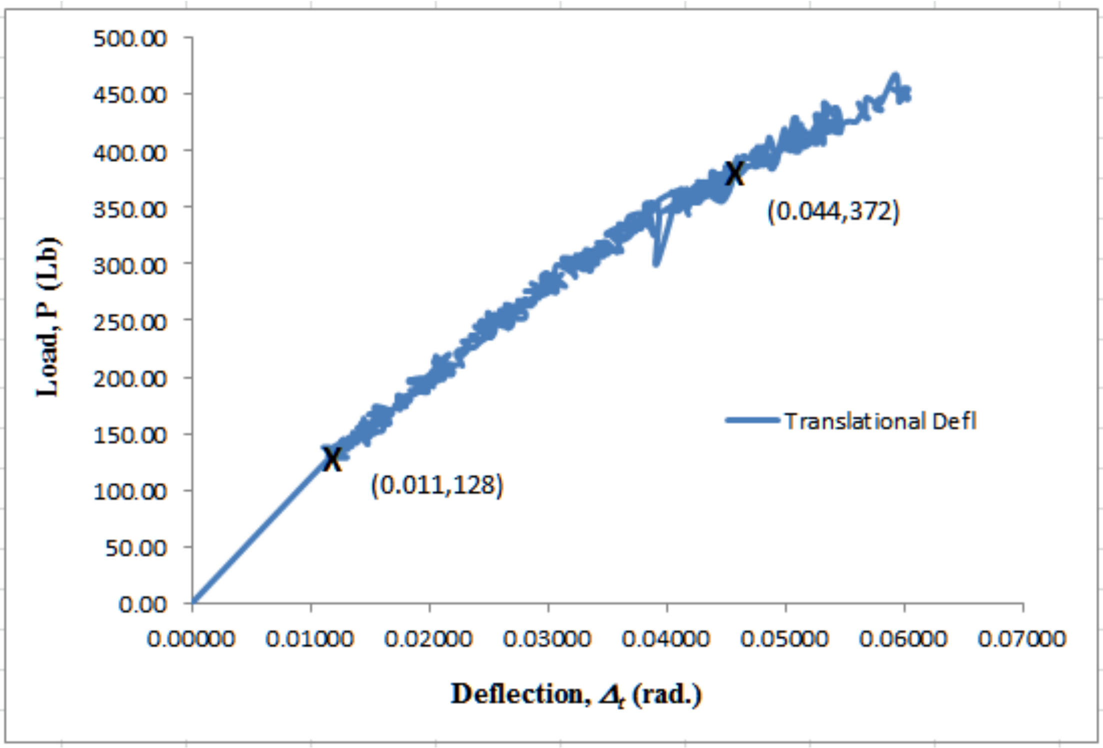

Figure 21: Force vs. Translational displacement for test C1